5-12-2023

Effects of biochar content and particle size on mechanical properties of biochar-plastic composites

Anne Marie Mozrall
amm2330@rit.edu

Effects of biochar content and particle size on mechanical properties of biochar-plastic composites

By

Anne Marie Mozrall

A Thesis Submitted in Partial Fulfillment of the Requirements for the Degree of Master of Science in Packaging Science

Department of Packaging and Graphic Media Science
College of Engineering Technology

Rochester Institute of Technology
Rochester, NY
May 12, 2023

ABSTRACT

The recent increases in plastic pollution and consumption have put bioplastics in a strong position to expand. However, better understanding is needed for bio-fillers and their effect on popular bioplastics, such as poly (lactic acid) (PLA), in order for this to occur. Biochar (BC), a stable form of carbon derived from high temperature conversion of organic material, has potential application as a plastic filler. Although biochar's effect on petroleum-based plastics has been widely studied, there are still major gaps in the literature surrounding biochar use as a filler in PLA/starch composites. Biochar particle size and loading are two factors that greatly affect a composites' mechanical properties. Thus, in this work, the effects of biochar particle size and biochar loading were examined when paired with a PLA/starch matrix. Mechanical and thermal testing was performed on composites that varied in filler loading (0-20 wt.%), as well as biochar filler particle size. At 20 wt.% biochar, the finer biochar particles produced a drop in the viscosity, which could be attributed to degradation within the composite at higher loadings. Mechanical characterization showed that increasing the BC filler loading, increased the modulus of elasticity. Decreasing the particle size also increased the modulus of elasticity, and therefore made the composite stiffer. The most prominent finding showed that through a combination of decreasing the particle size and identifying an ideal filler loading (5wt.%), we were able to double the tensile strength and slightly increased the elongation, thereby increasing the composites toughness. These results indicate that particle size and loading are important design consideration when using biochar as a filler.

ACKNOWLEDGEMENTS

I would like to acknowledge and show appreciation to my research advisor Dr. Carlos Diaz-Acosta, who made this work possible. His guidance and support carried me through all the stages of this research project. I would also like to thank my committee member, Dr. Thomas Trabold and Alexis Rich, for letting my defense be an enjoyable moment and for their time, support and suggestions.

Additionally, I would like to thank all those in Dr. Diaz's research group, especially Yvan Hernandez, who aided me with different portions of this work. Your efforts and time have not gone unnoticed.

Finally, I like would like to thank my friends and family as a whole, for their continuous support. I would not have been able to get to this point without them.

TABLE OF CONTENTS

LIST OF TABLES

LIST OF FIGURES

Chapter 1: Introduction

Plastic pollution is a growing problem that has been at the forefront of public discussion over the past several years [1]. Recently, this problem has continued to grow as Covid-19 spiked the need for individually packaged products and single use plastics [2]. Many organizations are actively working to mitigate this issue. One response from major brand owners has been pledging support to initiatives put forth by the Ellen MacArthur Foundation and similar institutions. Companies have also announced public goals vowing to reach certain milestones related to plastic use, in an effort to create a circular economy and reduce the amount of virgin plastic used. For example, PepsiCo has pledged to eliminate 400,000 metric tons of virgin material by 2030 [3]. One way to accomplish these initiatives is through the development and testing of new materials that offset virgin plastic use. Biochar (BC) is a stable form of carbon, produced by high temperature conversion of biomass in an oxygen limited atmosphere, that can replace common plastic fillers such as carbon black and calcium carbonate, $CaCO_3$ [4]. BC has been studied as a filler in a wide variety of composites, including bioplastics. Bioplastics can be derived from varying renewable resources and can offer alternative end-of-life scenarios such as composting and biodegradation. These alternatives provide new end-of-life pathways for packaging that traditionally ends up in landfills [5].

One specific bioplastic that has been widely studied is poly (lactic acid) (PLA). PLA has great potential to be a bio-based alternative, due to its excellent mechanical properties and industrial viability [6]. For example, Haelderman et al. [6] evaluated PLA/starch composites containing BC and the filler's effects on the thermal properties. Additionally, Aup-Ngoen and Noipitak [7] studied PLA/BC composites and how the mechanical properties were affected when the BC was derived from different biomasses. Although PLA alone has been widely researched, there are still gaps in the literature regarding PLA, starch and biochar composites. Additionally, there is currently a lack of research on how BC particle size can affect the PLA/starch composite properties.

In two previous studies by Diaz et al. and Mozrall et al. [8], [9], similar work was conducted. Diaz et al. examined the mechanical properties of PCL/starch/biochar using coffee ground biochar. However, the effect of particle size was not examined [9]. Mozrall et al. was a preliminary study that studied PLA/starch/BC in comparison with other matrices to find a composite with similar characteristics to cardstock[8]. PLA/starch has been chosen as the matrix material for the current research, because of its brittleness and the improvement potential in the tensile properties. Based on existing literature, PLA and starch are known to be brittle materials,

and typically adding additional fillers can increase this brittleness. However, it has been found that the right combination of filler loading and particle size, can result in the increase in toughness. This hypothesis is supported by previous work done by Peterson and Kim [10], who conducted a study that used nanosilica as a co-milling material to decrease the size of BC particles. The study found that co-milling the BC, to decrease the particle size, led to no loss in tensile strength and an increase in elongation and toughness [10].

Based on the above logic, the goal of this study was to create a bio-based alternative to traditional petroleum plastics, that not only offsets virgin plastic use, but is derived for renewable resources. This study assessed PLA/starch/BC blends that varied in BC loadings and BC particle size in an effort to increase the strength and elongation potential of the composites.

Chapter 2: Literature Review

2.1 What is Biochar?

Biochar (BC) is defined as a "carbon-rich material with a porous structure, mainly made up of aromatic hydrocarbons and graphite-like structures" [11], that is made from organic biomass in a process called pyrolysis (see section 2.3). BC, as mentioned previously, is being researched as a potential filler for plastic and bioplastic composites. BC not only has the potential to displace traditional plastic use and repurpose organic material waste, but also has been found to increase degradation rates of certain plastic composites and contributes to a more circular economy [12]. These factors have led researchers to take a closer look at BC use in plastics and bioplastics. Additionally, due to its porous structure, BC has been utilized in a variety of different settings [11]. BC was originally researched to act as an agent for carbon sequestration potential and soil remediation [10], [13]. In addition, BC has also been used as a absorptive media for pesticides, herbicides and heavy metals [10]. BC has been somewhat successful in these other areas; however, researchers are still trying to uncover what untapped potential BC might have in plastics and polymers, and other manufactured products. Carbon black is one of the main materials BC is being researched to replace.

2.2 What is Carbon Black?

Carbon black has been widely used and studied for over 50 years [14]. As of 2019, 8.1 million metric tons of carbon black are produced per year, making it one of the top 50 global industrial chemicals [15], most of which is used by rubber and elastomer manufacturers [14]. Carbon black is very porous and has a large surface area, making the material widely successful as a rubber and plastic filler [15].

Currently, the process of making carbon black is extremely energy intensive and expensive. In order to make carbon black, combustion of heavy hydrocarbons occur and hydrocarbon oil or natural gas is used as the feedstock. It is estimated that 30-35% of the price of carbon black comes from the feedstock price and with oil prices rising, the price of carbon black is not anticipated to go down. Additionally, for every 1 ton of carbon black that is produced, 2.4 tons of carbon dioxide are emitted [15]. Finally, a petroleum based composite is typically nondegradable, making composites that use carbon black incompatible with a circular economy [15].

2.3 Pyrolysis

Pyrolysis is typically defined as thermal decomposition of organic compounds/biomass without oxygen and is one of the ways in which biomass is converted to energy. The process of pyrolysis produces a liquid bio-oil, a char and gaseous byproducts [16]. The quality of BC byproducts is dependent on the material it is made from, as well as the parameters of the pyrolysis. Changing variables, such as temperature, heating rate can lead to an increased yield or higher quality char [17]. There are three main types of pyrolysis, slow, fast and flash pyrolysis, all of which produce varying amounts of biochar [16]. Each method of pyrolysis will yield different amounts of each pyrolysis byproduct. Typically, slow pyrolysis has shown to produce the highest biochar yield [17]. Slow pyrolysis is currently commercially used for the creation of charcoal, however with the increasing amounts of research being done on biochar, a commercial need for the pyrolysis of biochar could come soon [16].

2.4 Effect of feedstock on biochar

BC can be made from a wide variety of organic and carbon rich feedstocks such as grasses, coconut shucks, wood chips and coffee grounds [11], [13]. Different feedstocks produce biochar with different characteristics, which can be tailored to specific applications [13], [16]. For example, Hernandez-Charpak et al. [13]conducted a study comparing dairy manure BC to wood chip BC. The study found several differences between the two BC samples. The dairy manure BC was found to have a higher moisture content and pore radius, whereas the wood chip BC had a larger surface area. Hernandez-Charpak et al. also paired the BC with varying matrices such as; polypropylene (PP), polycaprolactone (PCL) and PLA and examined the thermal and mechanical properties. The study found that the tensile strength, elongation at break and thermal behavior were all affected by BC feedstock, and specifically more affected by the BC moisture content [13]. Additional factors that can affect BC properties are feedstock particle size, biomass pretreatment, and biomass carbon content [7], [16].

2.5 Composites

In a packaging application, BC from varying feedstocks, has been coupled with a wide variety of materials such as rubber, starch, nylon, fiberglass, traditional plastic composites and bioplastic composites. The material to which BC is added is referred to as the matrix material. Based on a literature review, composites exhibit different properties based on matrix material, biochar feedstocks and biochar processing [4], [9], [13], [17], [18]. For example, Hernandez-Charpak et al. examined biochar feedstock paired with different matrices (PLA, PP and PCL)

and found that matrices that were more susceptible to hydrolysis were more sensitive to BC with higher moisture content [13]. Das et al. studied waste biochar mixed with PP as a compatibilizer [18]. Aup-Ngoen and Noipitak found that mixing BC with PLA showed an improved modulus of elasticity and an increased in the impact energy [7]. Although these studies focused on different applications, their matrix choice had an effect on the results. Biochar that is added to a rubber matrix, might not show the same results when compared to a bioplastic such as PLA.

2.6 Bioplastics and PLA

As previously stated, BC has been studied in a wide variety of composites, including bioplastics. Bioplastics are plastics derived from renewable resources such as corn, sugar or potatoes [5]. Currently, one of the most widely used bioplastics is PLA because of its favorable properties, such as being made from renewable resources, biodegradability, industrial viability and economically viable synthesis processes [6], [7], [19]. However, PLA has several drawbacks that do not allow it to be as widely used, compared to typical petroleum-based plastics. PLA alone is very brittle and lacks the toughness required to be used in many applications outside of food packaging, 3D printing and textile fibers [6], [7]. Fillers have been used with PLA to mitigate some of these issues and reduce costs [7]. Starch is a common filler paired with PLA because it is is relatively inexpensive and easy to source. Since starch is also a biobased material, combining starch with PLA allows the composite to remain biobased [19]. Additionally, when added to PLA, starch helps to improve the toughness [6]. Biochar has also been used as an individual filler in PLA, but the literature discussing the combination of biochar and starch as fillers together, still has gaps. Haeldermans et al. examined PLA/starch/BC composites when compared to PLA/starch and PLA/BC composites, but focused mainly on thermal characterization and higher loading of BC (20-50 wt%) [6]. Additionally, this study looked closer at how the matrix and two fillers interacted with each other, rather than the performance of the composite as a whole [6]. One interesting outcome from this study was that the starch and BC have no influence on the glass transition temperature [6]. However, the study did not consider particle size in its experimental campaign.

2.7 Filler Loadings

In addition to the matrix/filler material affecting the overall composite properties, the filler loading can also affect the properties a composite exhibits [20]. Increased amounts of filler have been shown to alter the composites tensile and thermal properties [20]. For example, Zhu et al. found that when creating a polyimide/silica composite, the strength and the elongation

increased with a particle loading up to 10 wt%, but any additional loading caused a decrease [21]. Additionally, Fu et al. demonstrated that increasing the filler loading can also increase the modulus of elasticity. The study also discussed how adding inorganic fillers, where the particles are poorly bonded to the matrix, can decrease the tensile strength [22]. Since PLA has traditionally been too brittle for widespread industrial use, examining how increasing amounts of BC filler affect the composite properties is vital for overall understanding and maximum virgin plastic offset.

2.8 Particle Size

The particle size of the BC can affect the matrix/filler interaction as well as the mechanical and thermal properties of the composite. Currently, particle size is one reason BC is not as competitive with carbon black. Carbon black typically has a particle size distribution ranging from 10 to 500 nm [15]. Biochar usually has particles larger than 10 µm, depending on the feedstock and any additional grinding methods used, making even ground BC particles orders of magnitude larger than typical carbon black particles.

BC particle size has been studied in some applications with varying matrices, but not when incorporated with PLA and starch. A study done by Huber et al. [23] studied the effect of BC particle size on the viscosity of nylon composites. The study used ball milling for different lengths of time and examined BC with particle sizes ranging from 0.5 to 10,000 µm, broken down into different size ranges. The study concluded that ground BC appeared to have a dramatic effect on the flow behavior and viscosity of the composites [23]. Additionally, the study predicted that the BC particle size would impact the tensile and flexural strength of a polymer composite, since these mechanical properties are greatly influenced by interface adhesion. Interfacial adhesion and reinforcement can be expected to increase, as the BC particle size decreases, due to the increase in surface area[23].

Peterson and Kim [10] conducted a study to assess the effect of BC particle size on the mechanical properties of rubber composites. The particle size achieved through milling had a range from 0.075 to 1.5 µm [10]. The study found that co-milling the BC with nano-silica, to decrease the particle size led to no loss in tensile strength and an increase in elongation and toughness. However, the study did state that larger particle sizes of any fillers have been shown to reduce the reinforcement properties of rubber composites.

Dittanet and Pearson [24] found that the literature on the effect of particle size has contradicting views. Although this study looked into epoxies rather than thermoplastics, they demonstrate that there is still a need for data showing the effects of particle size on the

mechanical properties of BC composites. They highlighted that certain studies have reported a decrease in particle size increases the interfacial area and thereby increases the strength of a composite, whereas other studies have found that this decrease in particle size has no effect. The contradictory literature draw light to the need for further research on BC particle size.

2.9 Mixing and Torque

On a small-scale, samples are compounded in a high shear internal mixer such as CW Brabender 3-piece mixer. The mixer is connected to a torque rheometer which could also drive other attachments, ranging from a single chambered mixer to a twin-screw extruder. The instrument is able to record the torque at different stages while a composite is undergoing mixing. These values are recorded on a plastogram that plots the torque and the temperature of the composite while it undergoes mixing. Two values of importance from the plastogram are the maximum torque and the equilibrium torque.

The maximum torque can also be referred to as the fusion torque. When the torque reaches a maximum, it is thought to be the point where the composite is in a void-free state. Here, melting is occurring where the composite meets the hot metal surface [25]. An increasing shift in the maximum torque can be attributed to "a gelation of both agglomerates and primary particles progressing" [25].

The equilibrium torque is another value indicated on a plastogram during mixing. The equilibrium torque marks the end of the mixing process where a homogeneous mixture is achieved. The torque reaches a peak (the maximum torque) and then slowly levels out and comes to a steady state which is the equilibrium torque [26]. Equilibrium torque is a value that is often used to give insight into the composite's viscosity. A lower equilibrium torque infers a lower apparent viscosity.

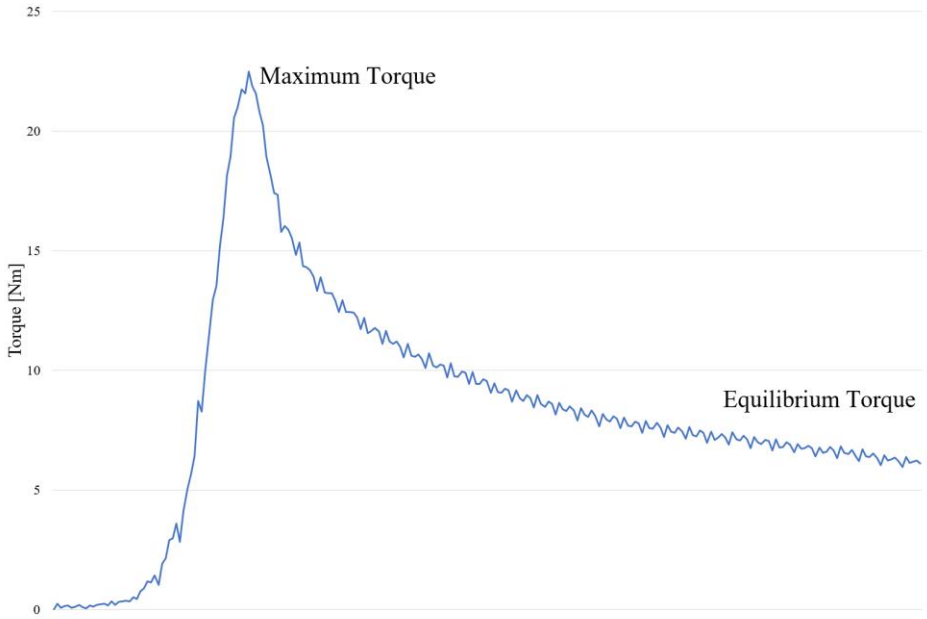

***Figure 1**: Sample plastogram with indicated max and equilibrium torque*

2.10 Particle Size Reduction

BC particle size can be reduced through different milling techniques, such as ball-milling, hammer milling, cryo-milling, disk milling, centrifugal mill, etc. [27]. Hammer milling and cryo-milling were the two techniques used in this study. Hammer milling decreases particle size by crushing the feedstock particles with rotating blades that are then pushed towards the bottom of the mill and through a screen. If the particles are not small enough to pass through the screen diameter, then they will continued to be ground until they reach the desired diameter [28]. Cryo-milling or cryo-grinding, uses liquid nitrogen, along with a metal rod or ball to crush chilled content. Cryo-grinding is currently not economically viable on a commercial scale, due to the high cost of liquid nitrogen and the small amount of material produced [29].

2.11 Mechanical Testing

Mechanical testing is one of the main evaluations for rigid and semirigid composite materials. A machine equipped to deliver constant-rate-of-crosshead-movement coupled with a load cell is used to acquire force as a function of deformation, which gives insight into the materials strengths and weaknesses. The tensile properties are obtained in accordance with standard ASTM-D638, specific for sheet, plate or molded plastics. These plastics are categorized into five types, which dictates what kind of dog bone shape they should be molded in for testing [30].

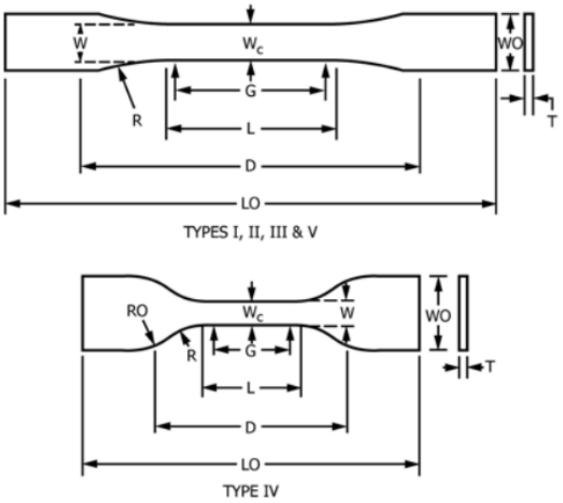

Figure 2: *Example of dog bone shape and what types use each taken from ASTM-D638*

For this study, a type V dog bone was used. Type V has smaller dimensions but the same shape as Types I, II and III. The dimensions of the all types can be found in the standard referenced above. Once testing is complete, there are several values that can be obtained from the stress/strain plot that is created. Three that are typically used are the modulus of elasticity, tensile strength at maximum force, and the tensile strain at break. The modulus of elasticity describes a material's ability to resist deformation and gives insight into the composite's stiffness [22]. The modulus is calculated by finding the slope on a stress-strain curve in the elastic region [30]. The tensile strength describes the amount of stress a material was able to withstand prior to breaking. Finally, the tensile strain describes the amount of elongation a material reaches prior to breaking and gives an indication of the ductility of the sample.

2.12 Scanning Electron Microscopy

Scanning electron microscopy (SEM) is a technique used in many disciplines, to visualize surfaces at magnifications higher than those achieved by optical microscopes. The average range of magnification achieved through SEM is 5x to 300,000x [31]. SEM can be used on both organic and inorganic materials, which is one of the reasons it is so valuable when examining polymer properties [31]. SEM technology achieves this level of magnification through the emission of electrons. The electrons hit the surface of the material, which is typically sputtered in gold/palladium and bounces off creating a grey scale image [31]. The sputtering and the SEM scanning are both done in a vacuum; however, the sputtering requires a means of transfer so argon is typically used. Sputtering is only done in order to make a composite conductive on the surface that is being captured; this is what allows the electrons to bounce off the composite.

2.13 Thermal Testing

There are several kinds of thermal analysis that can be conducted on polymers. Differential scanning calorimetry (DSC) is an analytical technique, developed in the early 1960s, used to determine various melting, crystallization and transition temperatures [32] and is a common tool for polymer analysis. It can also be used to determine if there is degradation within a composite or film by putting the sample through multiple heating and cooling cycles. DSC tends to have a wider range of heating and cooling rates compared to other calorimetric tools [32].

Chapter 3: Methodology

3.1 Materials

Poly (lactic acid) (PLA) 4043D was obtained from NatureWorks (Minnetonka, Minnesota, USA). Cornstarch was obtained from MP Biomedicals (Solon, Ohio, USA). The BC was fabricated from waste coffee grounds acquired from the Rochester Institute of Technology (RIT) cafeteria and first dried using an in-house batch dehydrator (Ecovim-250, Ecovim USA, Los Angeles, CA, USA). Then the materials were processed in a commercial scale “Biogenic Refinery " made by Biomass Controls (Woodstock, CT, USA) and owned by RIT. To turn the coffee grounds into BC, the dried material was fed through a hopper and auger assembly at an average flow rate of approximately 5kg/h. As described by Diaz et al. [9], the temperature setpoint was maintained at 800°C ± 25°C over the course of approximately a three-hour long experiment. After the thermochemical conversion was completed, a dual auger system transported the BC to the collection box, where the BC was quenched with water to cool the material down and to stop any further reaction with the ambient air.

3.2 Design of Experiment

The effects of particle size and BC content were evaluated in the context of a full factorial design of experiments (DOE), which can be seen below in Table 1. BC loadings was a continuous factor and was studied in the range of 0-20 wt. %. These weight fractions were selected based on previous research and difficulty when trying to add more than 20 wt.% BC, due to a drop in the composites viscosity while mixing. The particle size was a categorical factor with three levels based on different grinding techniques: unground, Thomas Scientific Wiley Mill (TSWM) and cryo-milled. A factorial analysis was performed on all data points to confirm statistical significance. Interval and interaction plots were calculated for each set of data to 95% confidence.

Table 1: *Sample composition and DOE sample preparation order*

Std Order	Run Order	PS Grinding Method	BC Filler Content (wt.%)
23	0	Control-1	0
15	1	Unground-1	15
7	2	TSWM-1	15
8	3	TSWM-1	20
20	4	TSWM-2	20
18	5	TSWM-1	10
11	6	Cryo-mill-1	15
19	7	TSWM-2	15
2	8	Unground-1	10
23	9	Cryo-mill-2	15
17	10	TSWM-1	5
16	11	Unground-1	20
13	12	Unground-1	5
4	13	Unground-2	20
1	14	Unground-2	5
24	15	Cryo-mill-1	20
6	16	TSWM-2	10
14	17	Unground-2	10
3	18	Unground-2	15
5	19	TSWM-2	5
12	20	Cryo-mill-2	20
9	21	Cryo-mill-1	5
21	22	Cryo-mill-2	5
10	23	Cryo-mill-1	10
22	24	Cryo-mill-2	10
24	25	Control-2	0

3.3 Biochar milling

Different particle sizes of BC were obtained by utilizing three grinding methods. The first sample was used as received and it is referred to as the unground PLA/starch/char samples. The same unground BC was then put through different grinding methods, to further reduce the particle size for the additional samples. The second sample was ground in a Model 4 Thomas Scientific Wiley Mill (Wiley Mill, Thomas Scientific, Swedesboro, NJ). The hammer mill feeds the raw material through a hopper into a series of rotating blades. The blades crush the raw material and the particles through a 1mm screen beneath the blades.

The third sample was ground in a 6875 Freezer/Mill High-Capacity Cryogenic Grinder (cryo-mill). The cryo-mill is a cryogenic grinder that contains one dual chamber, in which samples are continuously submerged in liquid nitrogen to maintain cryogenic temperatures. 30-35 grams of unground BC were placed in the cryo-mill. Each sample underwent four cycles with a 10-minute precool, a 6-minute cycle time and a 3-minute cooling cycle. The cryo-mill had a rate of 15 rpms. The final sample is referred to as the cryo-mill sample.

3.4 Particle Size Distribution

To identify particle size, an Amscope ME520 series optical microscope was used with an MU900 camera and software version x64, 4.11.18573.20210303. Multiple micrographs were taken to get a representative sample. Fewer micrographs were needed to be taken of the finer samples, since more particles were captured in each image. Once an image was captured, a segmentation and count of the OSTU dark areas, using a circle as the approximated shape, was used to count the particles visible in each micrograph. A count result was used to generate the raw data that included the radius of each particle identified in the image. Histograms were generated in Excel using a log scale. Percentages of particles in the sample are based on particle area.

A second particle size distribution analysis was taken using a Meinzer II Sieve Shaker following American Society of Testing and Materials (ASTM) D2862-16. Seven sieves were used during this analysis, which had seven different screen openings. In descending order, the screen openings consisted of 1400, 850, 500, 250, 150, 90 and 10µm. A 50-gram sample of each of the BC samples was placed in the top sieve and then shaken for 10 minutes. After 10 minutes, the remaining BC in each sieve was collected and weighted. The weight of each sample was used to calculate the percentage of the total sample each particle size made up. The resulting distribution is therefore based on weight rather than particle area.

As previously mentioned, the particle size distribution calculated from the microscope was based on the particle area, whereas the particle size distribution calculated from the sieve shaker was based on weight. These two are different calculations and therefore produce slightly different results, however this is why having both is beneficial when trying to create a complete picture of the particle size distribution of each sample.

3.5 Composites Preparation

The plastic matrix and the BC filler were compounded using melt mixing methodology, followed by laser cutting into an ASTM dogbone shape, which can be seen in Figures 2 and 3. Each sample was made from 50 grams of material total, with relative amounts of filler and matrix outlined Table 1. Based on our previous work [8], the appropriate PLA/starch ratio was determined to be 63.9% PLA and 36.1% starch. Briefly, melt mixing was conducted in a high shear 60cc 3-piece mixing head CW Brabender (South Hackensack, NJ, USA) connected to an Intelli-torque Plasticorder torque rheometer. PLA/starch composites were blended in the mixer at 180 °C for 8 min at 15 rpm. All materials were dried at 50°C for at least 24 hours, prior to and after mixing in order to remove any moisture from the materials being used.

Building off the preliminary study, the speed of the mixer was dropped from 30 to 15 rpm. During preliminary testing, samples containing 20 wt.% cryo-milled biochar experiences a large drop in viscosity, leaving the composite almost completely liquefied at the end of the mixing process. By decreasing the speed of the mixer, the composite experienced a slightly lower shear stress.

After the composites were evenly mixed, the hardened mixture was transferred to a Carver Press (Model 4391, Wabach, IN, USA). Here the composites were pressed between two Teflon sheets for 10 min each with pressure between 3 and 4 tons at a temperature of 180°C, and then cooled by air and water through the platens. All samples were processed the same way except for the cryo-milled samples with a 20 wt.% loading of BC. These samples experienced a slight drop in torque during the mixing process and needed to be pressed at 1 ton in order to retain the integrity and thickness of the sample so it could be laser cut. The plastograms of all samples can be found in Appendices.

Once pressed into a flattened sheet, the samples were laser cut using a Full spectrum P-series P48, 90-Watt CO_2 laser 10.6 µm wave length. The specific machine used a power setting of 14 and a speed of 100 to perform the cuts; the resulting dog bones can be seen in Figure 3. Eight dog bones were cut from each sample, in order to complete mechanical analysis.

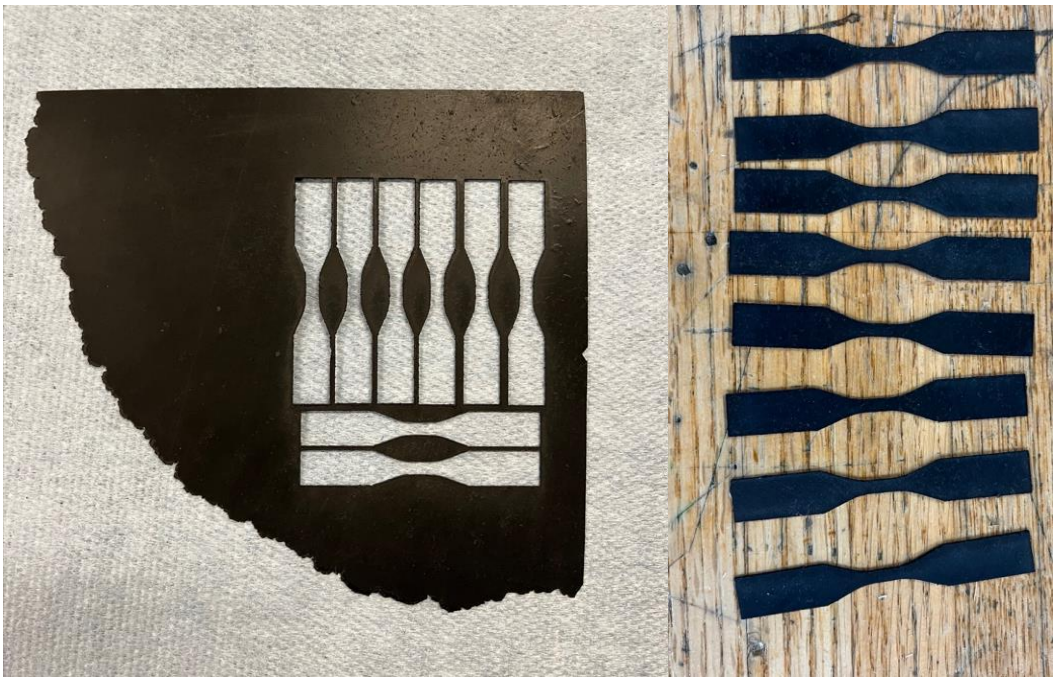

Figure 3: *Dog bone created by laser cutting after composite pressing*

3.6 Mechanical Properties Characterization

Tensile testing was conducted in an Instron (Norwood, MA, USA) Universal Testing Machine model 5567 at a cross head speed of 1.0 mm/min. A minimum of five dog bones specimens were tested for each sample, but most had more than five samples tested. Each sample was tested according to the ASTM- D638. Prior to each sample being placed in the machine, the thickness of each dog bone was measured, using calipers, to the nearest thousandth of an inch.

3.7 Scanning Electron Microscopy

Scanning electron microscopy (SEM) (TESCAN, MIRA3) of selected cross sections were taken. A 10.00 HV beam intensity was used, from a working distance of 10.0 mm. The analyzed samples were the control sample, as well as each of the 5% BC samples. The cross-section gives insight into what the inner structure of the composites. Each sample was frozen using liquid nitrogen to obtain a brittle break. Next, each sample underwent gold/platinum sputtering for 90 seconds on a 90° stand. Finally, the samples were placed in the SEM machine and imaged at 350x, 1000x and 2000x magnifications.

3.8 Thermal Analysis

DSC analysis was performed on all the samples and duplicates, using a DSC Discover D250 under a nitrogen atmosphere with a flow rate of 50 mL/min. 7.0 to 8.0mg of each sample were massed out and used for the DSC analysis. All samples were put through two heatings,

using a heat/cool/heat procedure. Samples were first heated to 210℃ at a heating rate of 10℃/min to eliminate the thermal history. The samples were cooled down to 0.0℃ at a cooling rate of 5℃/min. The second scan was reheating to 210.00℃ at the initial rate. The glass transition temperature (T_g), the melting temperature (T_m) and the melting enthalpy (ΔH_M) of the first and second scan of each sample were obtained from the DSC and measured with the Trios software version 5.1.

Chapter 4: Results and Discussion

4.1 Particle Size Distribution

Figure 4 shows the particle size distribution by optical particle count. The unground sample had a higher percentage of large particles, and an overall wider particle size distribution. The TSWM ground samples were slight smaller than the unground samples, with fewer particles over 100 µm. The TSWM utilized a 1 mm (1000 µm) screen, so the difference noticed with the larger particles coincides with the screen removing larger particles. The cryo-mill has noticeably smaller particles, with a majority of particles being under 10 µm. Additionally, it can be noted that there are no particles over 100 µm. Figure 5 shows a 10x microscopic image of each of the different samples after grinding

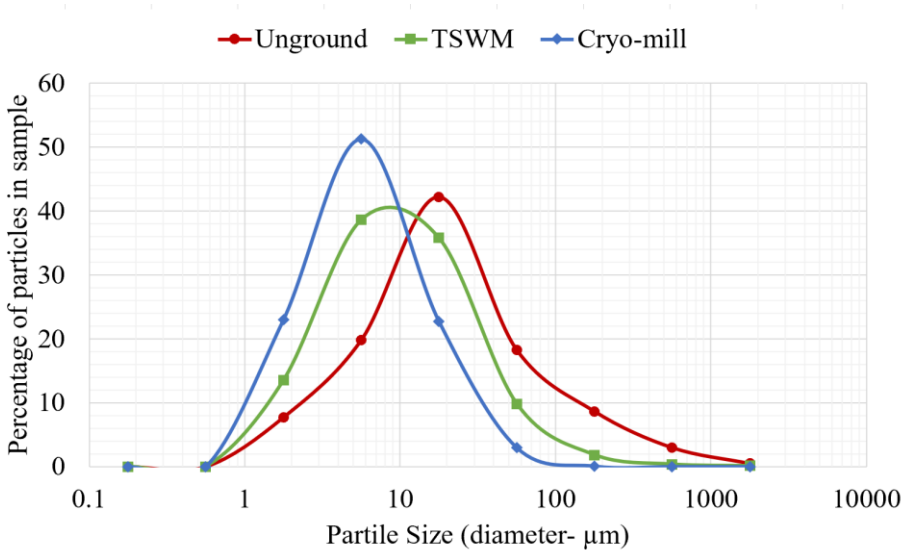

Figure 4: *Particle size distribution based on microscopic count*

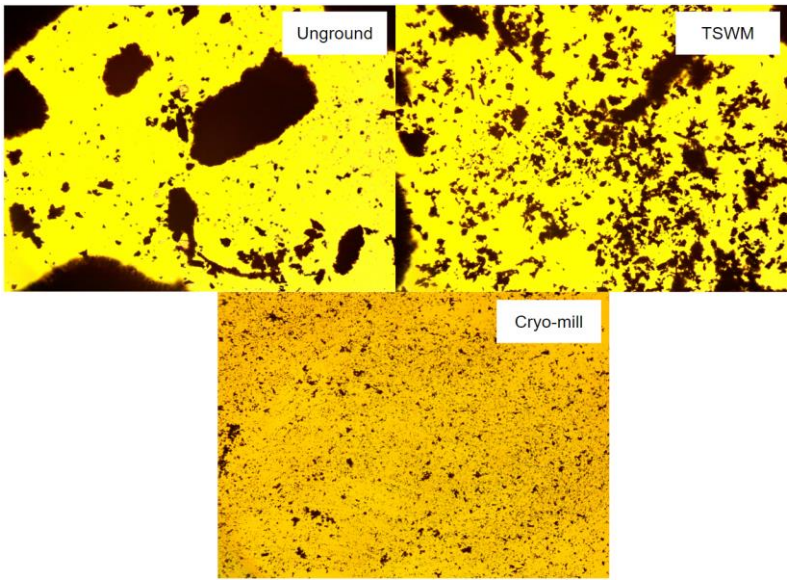

Figure 5: *10x images taken of each of the different samples*

Figure 6 shows the particle size distribution by weight. These results indicate greater differences between the three grinding methods. The unground sample is the only sample with particles over 850 µm, and with a majority of particles being over 500 µm. The TSWM ground sample has a majority of particles at or larger than 250 µm. Finally, the cryo-milled sample has a much narrower distribution of particles, with a majority of particles being 150 µm or less. Additionally, the cryo-milled sample has no particles over 500 µm.

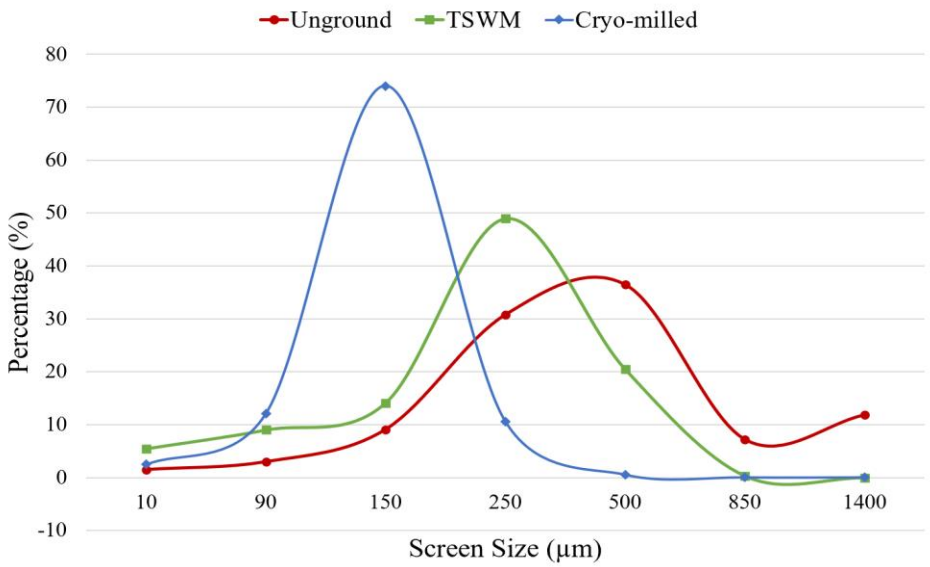

Figure 6: *Particle size distribution based on weight*

Based on visual observation, we believe that the two distribution methods are over estimating the particle size count, due to slight agglomeration of smaller BC particles. The agglomeration was most notably observed in the cryo-milled BC. The cryo-mill BC would stick together during optical counting and to the screens, when the mesh tower analysis was occurring, and therefore be counted in a larger particle size category. Figure 7 shows what is believed to be a cryo-milled BC agglomerations captured in a 10x microscopic image, as well as fine cryo-milled particles sticking to a larger mesh tower screen. All samples were dried before any testing to ensure that moisture content would not cause particles to stick together. The moisture content of the cryo-milled samples was tested and found to 6.84%. Another potential source of agglomeration is static within the samples. Although there may have been some agglomeration occurring prior to composite processing, the results confirm that the particles produced, from the three different grinding methods, are different in size.

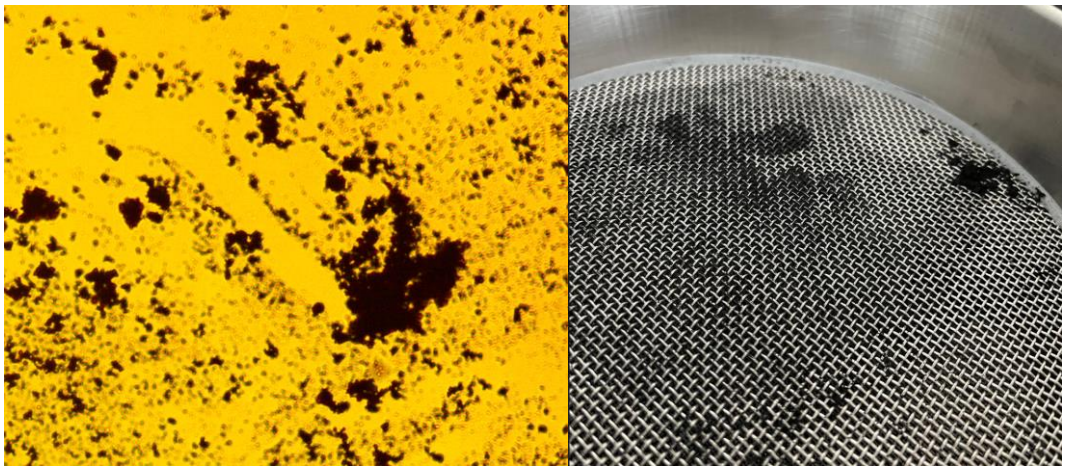

Figure 7: *Left: 10x cryo-milled BC agglomerations, Right: static agglomerations in screen following sieving*

4.1.1 Alternative methods of scaling up Cryo-milling

Cryo-grinding is currently not economically feasible on a commercial scale, due to the high cost of liquid nitrogen and the small amount of material produced per run [29]. However, there are some large-scale BC manufacturing companies sieving BC to separate the larger particles from the smaller. The larger particles are sold for uses such as cement and building materials, and the smaller ones are sold for lab research. Below, sieved woodchip BC from Aries Clean Energy, was compared to lab cryo-grinded biochar, through a particle distribution by weight. It can be noted that cryo-milled biochar has a narrower particle distribution range, with a majority of particles at 150µm, whereas the sieved BC has a wider particle size distribution, but had more particles at and below 90µm. Knowing that similar particle distribution can be achieved, using methods other than grinding, supports this research and makes it more appealing when looking to scale-up for commercial use.

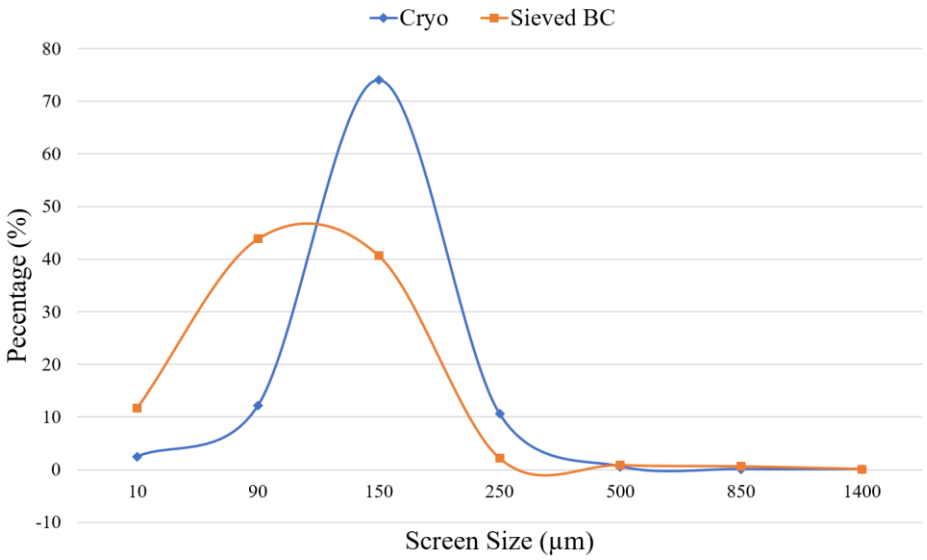

Figure 8: Particle size distribution by weight comparing sieved BC to cryo-ground BC

4.2 Scanning Electron Microscopy

Cross section SEM images were taken of a control sample as well as each the samples containing 5 wt.% BC. The entire cross section was examined under SEM magnification, prior to taking the images, to ensure all images taken were representative. Large honeycomb like structures can be seen in the unground and TSWM ground images; these structures are assumed to be BC. However, none of these structures can be seen in the cryo-milled images. Rather, there are much smaller specs seen in the cryo-milled sample, some of which can be assumed to be BC particles. The lack of visible BC structures coincides with the mechanical characteristics that are exhibited from the cryo-milled samples (refer to Section 4.5). The agglomerations that were seen prior to mixing, are likely broken up during processing, which is why only small BC particles can be seen in the cryo-milled sample.

BC agglomeration was discussed in the study of Bélanger et al. [33]. In which three different types of filler sizes were identified: agglomerates, aggregates and primary particles. Primary particles group to form aggregates, which can then also group to form agglomerates [33]. Carbon black is known to form agglomerates, but these tend to break down during mixing, whereas the aggregates do not. BC is known to also form agglomerates, but it is unclear whether these agglomerates break down during mixing or not. Based on the microscopic images (refer to section 4.1) and SEM images, there is agglomeration potentially occurring in all samples, but especially in the cryo-ground samples. SEM images taken at 1000x and 2000x can be found in

the Appendices. An image captured at 9000x of the cryo-milled sample can also be found in the Appendices that gives a clearer picture of the potential biochar specs.

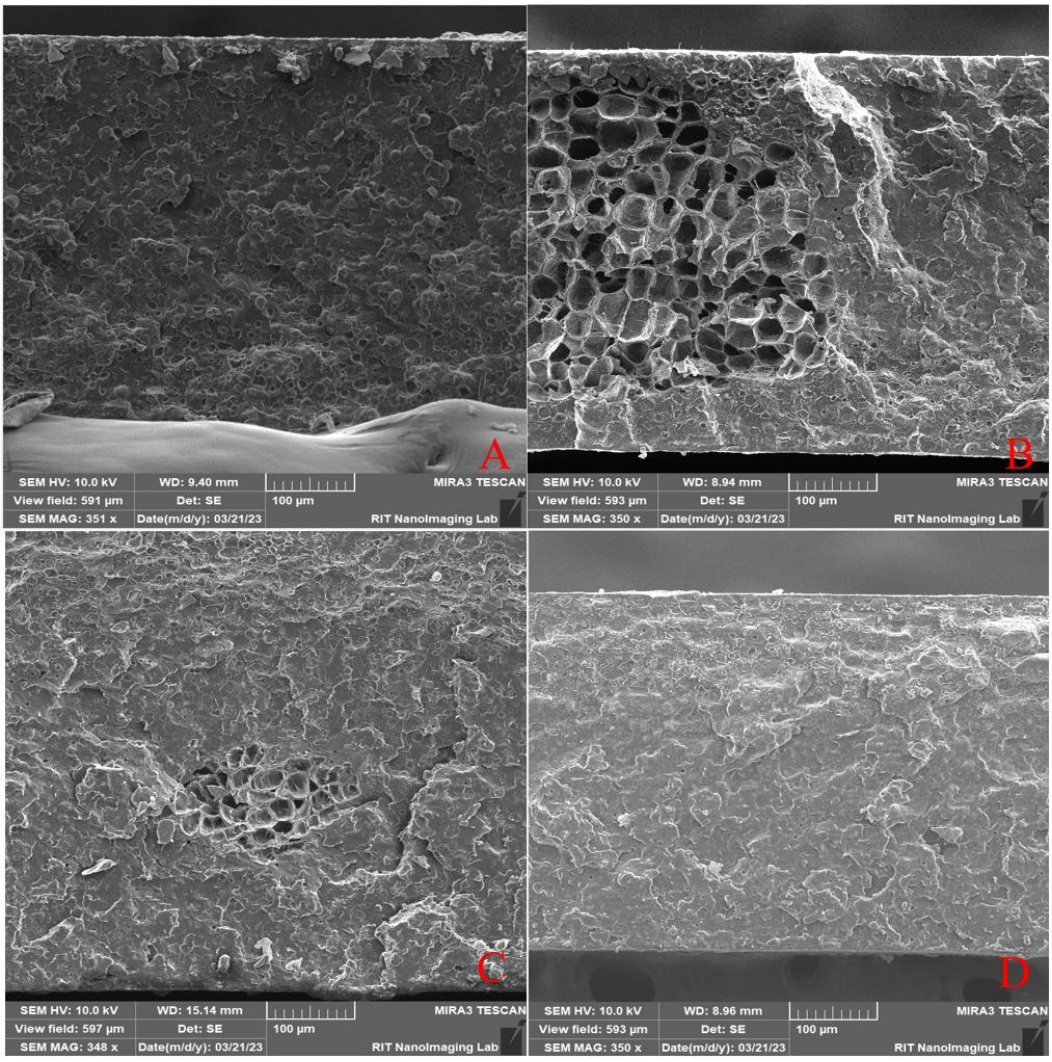

***Figure 9**: SEM images of samples taken at 350x magnification. Samples progress in the following order from left to right; Control (A), Unground 5% (B), TSWM ground 5% (C), Cryo-milled 5% (D)*

4.3 Effect of particle size on apparent viscosity

Figure 10 shows the equilibrium torque of samples containing 10 wt.% BC filler content. The equilibrium torque can give insight into the samples' apparent viscosity. At all loadings, samples exhibited similar patterns, where the unground and TSWM ground samples had a higher equilibrium torque than the cryo-milled. The plastograms of all the samples are compiled and shown in the Appendices organized by filler loading.

The data indicates that the samples with larger particles tend to have a higher equilibrium torque and therefore a higher viscosity, whereas the cryo-milled samples with smaller particles sizes, have a lower equilibrium torque. The fillers with smaller particles tend to have a higher surface area than those with larger particles. The larger surface area can cause more shear

between the matrix and filler while mixing, which can cause a drop in viscosity. A substantial drop in the cryo-milled samples' viscosity was observed at all biochar loadings. The 20 wt.% BC cryo-milled sample had the most dramatic decrease, with a final equilibrium torque being 2.5 Nm. A similar trend was observed by Hristov and Vlachopoulos in polyethylene composites with woodchip fillers. It was observed that at a 30% filler loading, the smaller particle fillers (75µm) had a lower shear viscosity than the larger particle fillers (250µm) [34]. Huber et al. also observed a similar trend in polyamide/BC composites, where the composite's viscosity decreased as the BC particle size decreased[23].

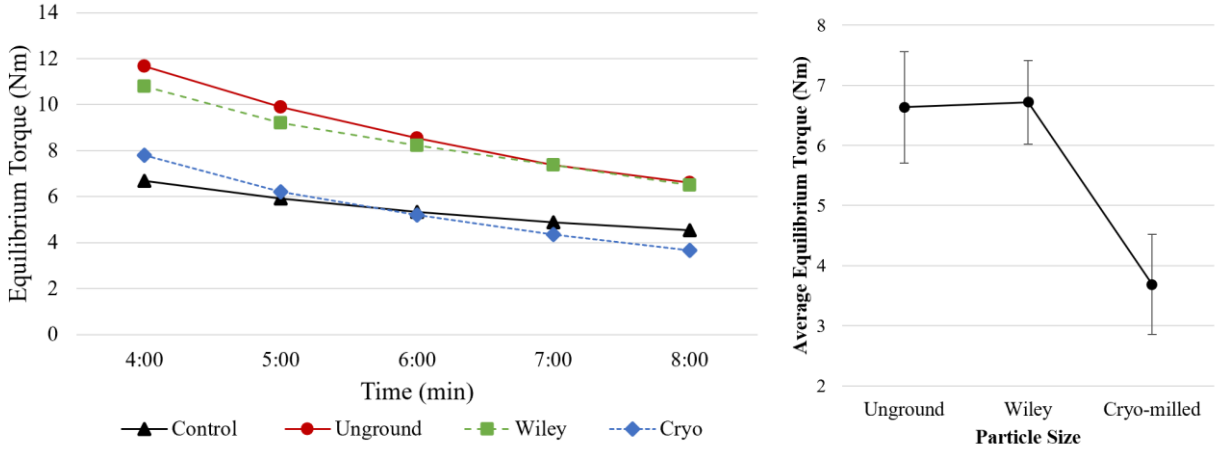

***Figure 10**: Left: Equilibrium Torque (Nm) of all samples containing 10% BC and control; Right: Interval plot of equilibrium torque vs. particle size*

In addition to comparing the equilibrium torque while mixing, the maximum torque was also examined (refer to Figure 11). The unground and TSWM samples had noticeably higher maximum torques than the cryo-milled samples. It can be inferred that the samples with larger particles required a higher torque for the samples to fully mix and for gelation to occur. Knowing the maximum torque is important for understanding the energy requirements of the samples being made. For machinery that has a lower threshold for torque mixing, a smaller particle samples would be better for continuous extrusion at lower torques.

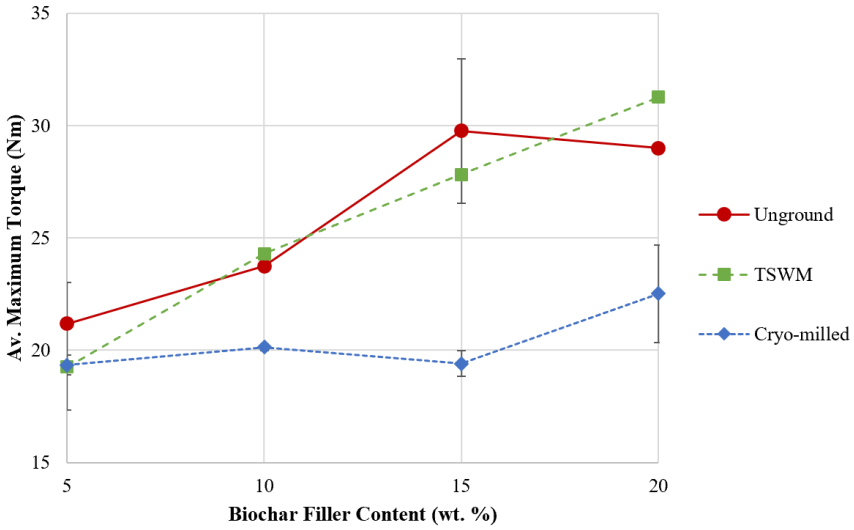

Figure 11: Interaction plot representing maximum torque in relation to BC loading and particle size

4.4 Effect of particle size on glass transition temperature

Table 2 depicts the glass transition temperature (T_g) of all the samples. A large drop in the 2nd heat glass transition temperature is observed in the 20 wt.% cryo-milled sample. In addition to the glass transition temperature dropping for the 20 wt.% cryo-ground samples, the sample did not exhibit a second heat enthalpy and instead exhibited enthalpy during the cooling cycle. No other samples experienced enthalpy during the cooling cycle. The drop in the glass transition temperature, coupled with the drop in the equilibrium torque (see section 4.3) experienced by the cryo-milled 20 wt.% samples, can indicate the composite is degrading while mixing. The lack of second heat enthalpy again point to the possibility of degradation in the sample during mixing, due to the higher shear stress caused by the increased amount of small particle filler. We hypothesize that the shear can leads to the degradation of polymer chains and polymer macromolecules or a loss of entanglement and molecular weight [34]. Haeldermans et al. also looked into glass transition temperature in varying loadings of PLA/starch/BC composites. The study looked at much higher loadings (20-50 wt.%), but did not consider the effect of particle size. Haeldermans et al. saw no drop in glass transition temperature as the loading increase, which is consistent with our results for the coarser BC [6]. Looking at these results and comparing them to our own, again infers that particle size is the factor causing the drop in glass transition temperature.

Table 2: *Second Heat Glass Transition (°C)*

Sample Name	Second Heat T_g (°C)
Control	58.25 ± 0.40
Unground 5%	57.67 ± 0.01
Unground 10%	57.85 ± 0.01
Unground 15%	56.61 ± 0.67
Unground 20%	56.20 ± 0.68
TSWM 5%	57.62 ± 0.32
TSWM 10%	57.58 ± 0.93
TSWM 15%	57.17 ± 0.24
TSWM 20%	57.41 ± 0.52
Cryo-milled 5%	58.37 ± 0.23
Cryo-milled 10%	57.06 ± 0.10
Cryo-milled 15%	57.41 ± 0.59
Cryo-milled 20%	53.62 ± 0.47

4.5 Effect of particle size on tensile properties

The tensile properties of all samples were examined through Instron testing and analysis. Table 3 shows all results and further discussion of individual properties is in the following sections.

Table 3: *Tensile Properties of all samples*

Sample Name	Modulus of Elasticity (MPa)	Tensile Strain at Break (%)	Tensile Strength at Max Force (MPa)
Control	790.00 ± 56.99	6.73 ± 0.53	27.84 ± 2.70
Unground 5%	795.63 ± 104.17	5.87 ± 0.68	20.45 ± 4.11
Unground 10%	718.83 ± 110.33	6.2 ±0.99	18.15 ± 4.77
Unground 15%	845.68 ± 106.63	4.54 ±0.43	18.36 ± 2.49
Unground 20%	901.34 ± 92.2	5.14 ± 0.42	16.96 ± 1.96
TSWM 5%	791.75 ± 65.21	5.78 ± 0.47	20.52 ± 3.04
TSWM 10%	747.22 ± 99.33	6.97 ± 1.09	20.85 ± 3.37
TSWM 15%	768.47 ± 79.25	6.37 ± 0.41	20.04 ± 4.07
TSWM 20%	820.91 ± 104.19	6.02 ± 0.36	17.20 ± 3.04
Cryo-mill 5%	930.36 ± 84.69	7.73 ± 0.57	42.89 ± 3.37
Cryo-mill 10%	976.06 ± 103.5	6.43 ± 0.33	33.81 ± 4.02
Cryo-mill 15%	940.41 ± 89.02	7.49 ± 0.83	32.89 ± 1.94
Cryo-mill 20%	1109.56 ± 167.20	4.88 ± 0.54	16.28 ± 3.17

4.5.1 Modulus of Elasticity

When examining the modulus of elasticity, it can be observed that the cryo-ground samples have a higher modulus of elasticity at all BC loadings. The unground and TSWM ground samples are relatively similar. At lower loadings (5 and 10 wt.% BC), both coarser samples have values lower than the control samples. At higher loadings (15 and 20 wt.% BC) the unground BC samples are higher than the control and at 20 wt.% the TSWM is also higher than the control. Since the modulus of elasticity is a measure of stiffness, the cryo-milled samples having higher modulus of elasticity indicates that the samples are stiffer at all loadings. Finally, it was observed that with all grinding methods, the samples with higher filler loadings have a higher modulus of elasticity.

The same effects have been seen in other studies. Fu et al. found that in nanoparticle polymer composites, as the filler loading increased, so did the modulus of elasticity. Although the study conducted by Fu et al. uses particles much smaller than the ones examined in this study, the same patterns are being observed with this research. Particles that remained unground or TSWM ground have similar modulus of elasticity, whereas cryo-milled samples have a drastically higher modulus of elasticity.

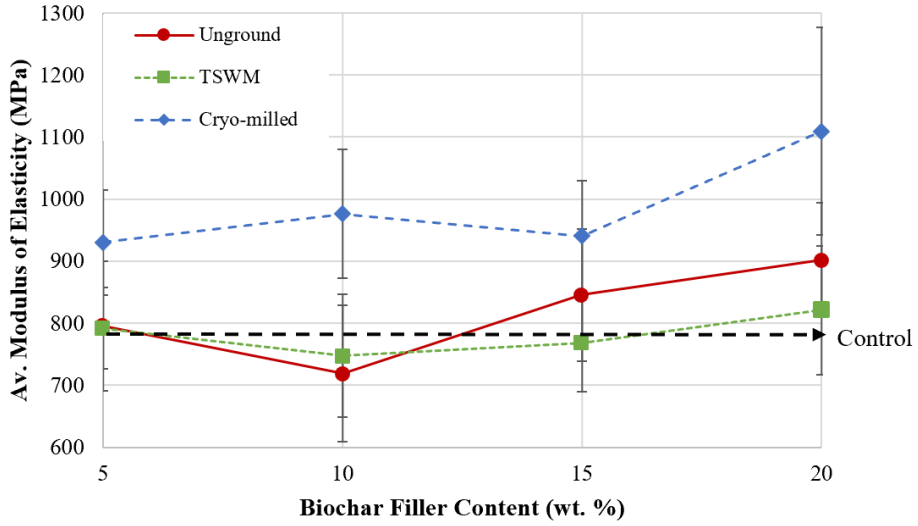

Figure 12: *Interaction plot of Average Modulus of Elasticity in relation to BC loading and particle size*

4.5.2: Tensile Strength at Max Force

Figure 13 depicts the average tensile strength of all the samples. The letters located next to samples represent groups that are statistically different. A one-way ANOVA was performed and the resulting p-value < 0.00. It can be observed that composites containing 5 wt.% cryo-

milled BC have a higher tensile strength than all other samples, followed by 10 wt.% and 15 wt.% cryo-milled composites. These three samples demonstrate higher tensile strength than the control sample, but the rest of the samples did not. In the two coarser BC samples, it can be observed that there was a loss of strength compared to the control. Generally, a drop in strength indicates there is poor interfacial adhesion [22]. With the finer cryo-milled samples we see a large increase in the strength compared to the control sample. The increase in strength can be attributed to the decrease in particle size and increase in filler surface area [10]. Additionally, we hypothesize that the particle size is influencing the adhesion with the matrix. However, additional testing would be required to confirm this hypothesis.

As the loading increases in the cryo-milled sample, a drop in strength was observed. The drop can be related back to the hypothesized degradation in the higher loading cryo-milled samples that was discussed early, specifically in the 20% cryo-milled sample; see Section 4.3 and 4.4.

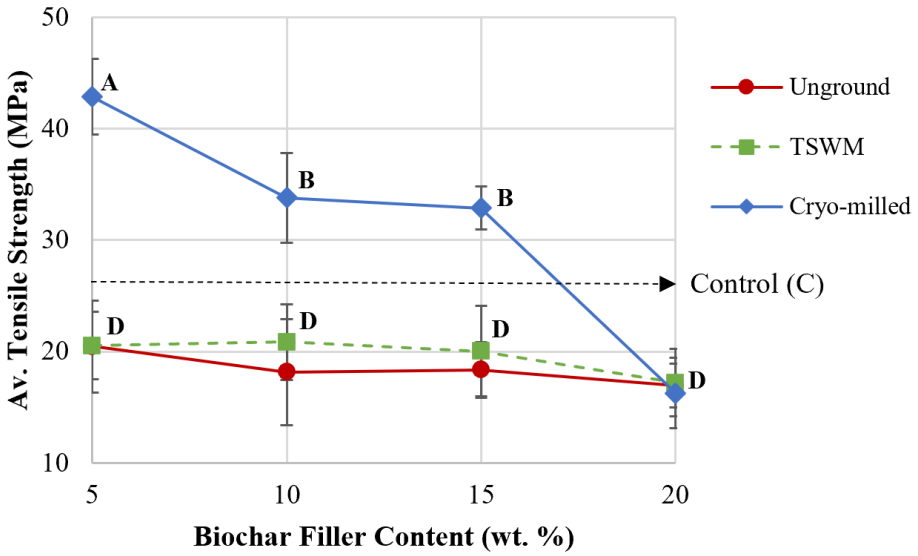

***Figure 13**:Interaction plot for Average Tensile Strength in relations BC loadings and particle size. Letter grouping represent statistically different data points*

Additionally, a peak was identified at 5 wt.% cryo-ground BC. An additional 2.5 wt.% BC sample was made with the cryo-milled BC and the strength was seen to be slightly lower, these results can be found in Figure 14. The peak again confirms that with right combination of filler loading and particle size a composite stronger than the control can be made.

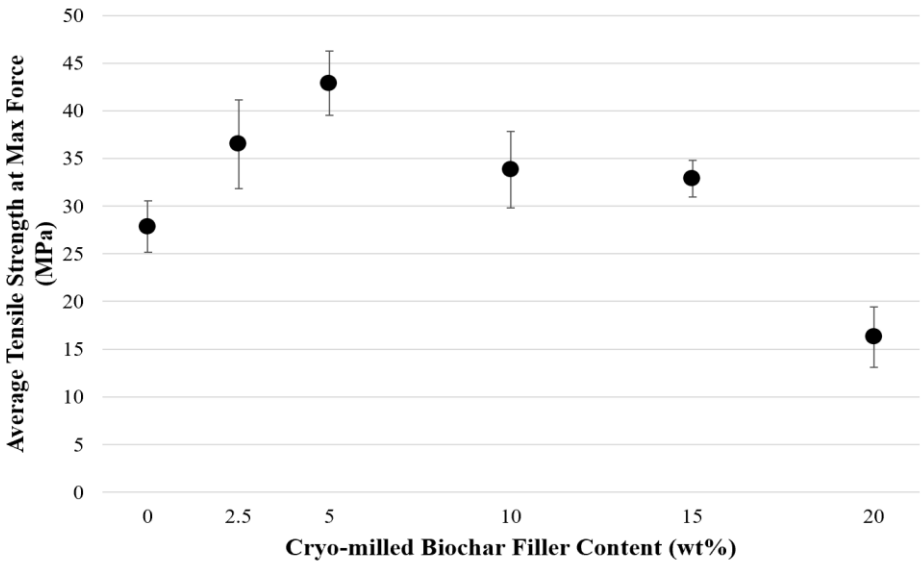

***Figure 14**:Cryo-ground Tensile Strength at Max Force (MPa) with added 2.5% sample to depict a peak identified at 5% BC*

4.5.3 Tensile Strain at Break

The full factorial showed little to no effect or interaction on the elongation of the composites. However, an ANOVA analysis of all the samples showed that the 5% cryo-milled sample was statistically higher than the rest of the samples. All of the samples are rigid composites and due to this, there will be very little elongation during the mechanical testing process. Based on the increase in tensile strength and the slight increase in elongation, it can be concluded that a formulation with increased toughness has been identified at 5 wt.% cryo-milled biochar loading[22].

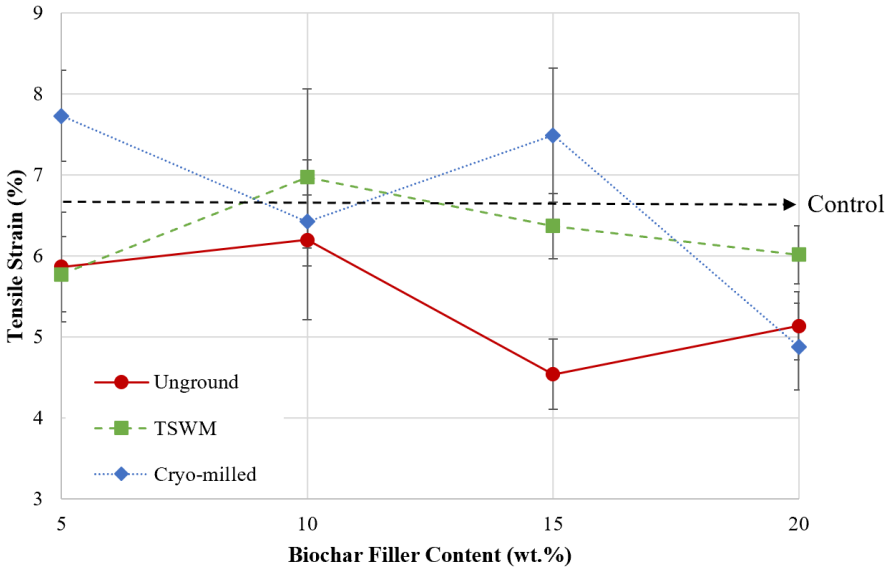

***Figure 15**:Interaction plot for Average Tensile Strain in relations BC loadings and particle size*

Chapter 5: Conclusion

Due to the recent interest in bioplastic, there has been a growing need to better understand bio-fillers and their effect on popular bioplastics, such as PLA. Biochar (BC), a stable form of carbon that can be derived from waste material, is also a widely popular alternative for petroleum based plastic fillers. Although BC has been widely studied, there are still major gaps in the literature surrounding BC used as a filler in PLA/starch composites. BC particle size and loading are two factors that are predicted to greatly affect a composite's mechanical properties.

This study looked at three different grinding methods to down size BC particle sizes for PLA/starch composites at different loadings. Particle size distributions were created using two different methods, one by optical count and another by weight. SEM imaging was taken of the cross section of specific composite samples. Additionally, DSC analysis was done on all samples to examine the glass transition temperature. Finally, mechanical analysis was done on all samples to examine and identify the desired tensile properties of the composites.

Several conclusions can be drawn from this work, the first being that the grinding methods used did in fact produce different particle size distributions. However, it was found that some static agglomeration occurred in the cryo-milled BC samples prior to mixing, which led to an overestimation of the particle size distribution. The lack of large BC structures in the SEM images of the cryo-milled samples supported this hypothesis.

When mixing the composites, it was concluded that the smaller particles cause a drop in the equilibrium and maximum torque. The smaller particles increased the amount of shear in the composite and there-by decreased the torque and apparent viscosity while mixing. The decrease in torque was greatest in the higher loading cryo-milled samples, specifically at a loading of 20wt.%. The potential degradation of the sample was again confirmed by a drop of the second heat glass transition temperature.

When examining the tensile properties, there were several findings resulting from both the BC loading and particle size. First, it was concluded that higher filler loadings increase the modulus of elasticity and therefore made the composite stiffer. Secondly, it can be concluded that particle size and increased filler surface area have an effect on the tensile strength between BC and the analyzed matrix. For the coarser BCs, there was an observed loss of tensile strength when compared to the control. However, as the loading decreased there was no additional loss in strength. The cryo-milled BC doubled the composite strength, when compared to the two coarser BC samples. This increase faded as the filler loading increased, which could be due to potential

composite degradation. Finally, a favored formulation was identified at 5 wt.% cryo-milled BC, since the strength and the elongation were both highest at this loading, inferring that the formulation increased the toughness of the composite.

References

[1] "Production, use, and fate of all plastics ever made | Science Advances." https://www.science.org/doi/full/10.1126/sciadv.1700782 (accessed Feb. 28, 2023).

[2] D. Sousa and F. D. Bastos, "Pros and Cons of Plastic during the COVID-19 Pandemic," *Recycling*, vol. 5, no. 4, Art. no. 4, Dec. 2020, doi: 10.3390/recycling5040027.

[3] "Packaging," *PepsicoUpgrade*. https://pepsico.com/our-impact/esg-topics-a-z/packaging (accessed Mar. 10, 2023).

[4] G. F. Ferreira, M. Pierozzi, A. C. Fingolo, W. P. da Silva, and M. Strauss, "Tuning Sugarcane Bagasse Biochar into a Potential Carbon Black Substitute for Polyethylene Composites," *J. Polym. Environ.*, vol. 27, no. 8, pp. 1735–1745, Aug. 2019, doi: 10.1007/s10924-019-01468-1.

[5] E. Bezirhan and H. D. Bilgen, "A Review: Investigation of Bioplastics," *J. Civ. Eng. Archit.*, vol. 9, pp. 188–192, Feb. 2015, doi: 10.17265/1934-7359/2015.02.007.

[6] T. Haeldermans *et al.*, "Poly (lactic acid) bio-composites containing biochar particles: effects of fillers and plasticizer on crystallization and thermal properties," *Express Polym. Lett.*, vol. 15, no. 4, pp. 343–360, Apr. 2021, doi: 10.3144/expresspolymlett.2021.30.

[7] K. Aup-Ngoen and M. Noipitak, "Effect of carbon-rich biochar on mechanical properties of PLA-biochar composites," *Sustain. Chem. Pharm.*, vol. 15, p. 100204, Mar. 2020, doi: 10.1016/j.scp.2019.100204.

[8] A. M. Mozrall, N. Eng, J. Brimlow, T. A. Trabold, and C. A. Diaz, "Effects of biochar content and particle size on the mechanical properties of biochar-plastic composites," in *30th IAPRI Member Conference*, Virtual: IAPRI, Jun. 2021.

[9] C. A. Diaz, R. K. Shah, T. Evans, T. A. Trabold, and K. Draper, "Thermoformed Containers Based on Starch and Starch/Coffee Waste Biochar Composites," *Energies*, vol. 13, no. 22, Art. no. 22, Jan. 2020, doi: 10.3390/en13226034.

[10] S. C. Peterson and S. Kim, "Reducing Biochar Particle Size with Nanosilica and Its Effect on Rubber Composite Reinforcement," *J. Polym. Environ.*, vol. 28, no. 1, pp. 317–322, Jan. 2020, doi: 10.1007/s10924-019-01604-x.

[11] Q. Zhang *et al.*, "Biocomposites from Organic Solid Wastes Derived Biochars: A Review," *Materials*, vol. 13, no. 18, Art. no. 18, Jan. 2020, doi: 10.3390/ma13183923.

[12] S. P. C. Gonçalves, M. Strauss, and D. S. T. Martinez, "The Positive Fate of Biochar Addition to Soil in the Degradation of PHBV-Silver Nanoparticle Composites," *Environ. Sci. Technol.*, vol. 52, no. 23, pp. 13845–13853, Dec. 2018, doi: 10.1021/acs.est.8b01524.

[13] Y. D. Hernandez-Charpak, T. A. Trabold, C. L. Lewis, and C. A. Diaz, "Biochar-filled plastics: Effect of feedstock on thermal and mechanical properties," *Biomass Convers. Biorefinery*, vol. 12, no. 10, pp. 4349–4360, Oct. 2022, doi: 10.1007/s13399-022-02340-4.

[14] K. Yurekli, R. Krishnamoorti, M. F. Tse, K. O. McElrath, A. H. Tsou, and H.-C. Wang, "Structure and dynamics of carbon black-filled elastomers," *J. Polym. Sci. Part B Polym. Phys.*, vol. 39, no. 2, pp. 256–275, 2001, doi: 10.1002/1099-0488(20010115)39:2<256::AID-POLB80>3.0.CO;2-Z.

[15] Y. Fan, G. D. Fowler, and M. Zhao, "The past, present and future of carbon black as a rubber reinforcing filler – A review," *J. Clean. Prod.*, vol. 247, p. 119115, Feb. 2020, doi: 10.1016/j.jclepro.2019.119115.

[16] T. Kan, V. Strezov, and T. J. Evans, "Lignocellulosic biomass pyrolysis: A review of product properties and effects of pyrolysis parameters," *Renew. Sustain. Energy Rev.*, vol. 57, pp. 1126–1140, May 2016, doi: 10.1016/j.rser.2015.12.185.

[17] R. Ibarrola, S. Shackley, and J. Hammond, "Pyrolysis biochar systems for recovering biodegradable materials: A life cycle carbon assessment," *Waste Manag.*, vol. 32, no. 5, pp. 859–868, May 2012, doi: 10.1016/j.wasman.2011.10.005.

[18] O. Das, D. Bhattacharyya, and A. K. Sarmah, “Sustainable eco–composites obtained from waste derived biochar: a consideration in performance properties, production costs, and environmental impact,” *J. Clean. Prod.*, vol. 129, pp. 159–168, Aug. 2016, doi: 10.1016/j.jclepro.2016.04.088.
[19] “Grafting of Glycidyl Methacrylate onto Poly(lactide) and Properties of PLA/Starch Blends Compatibilized by the Grafted Copolymer | SpringerLink.” https://link.springer.com/article/10.1007/s10924-012-0438-1 (accessed Feb. 28, 2023).
[20] J. Z. Liang and R. K. Y. Li, “Effect of filler content and surface treatment on the tensile properties of glass-bead-filled polypropylene composites,” *Polym. Int.*, vol. 49, no. 2, pp. 170–174, 2000, doi: 10.1002/(SICI)1097-0126(200002)49:2<170::AID-PI322>3.0.CO;2-U.
[21] Z.-K. Zhu, Y. Yang, J. Yin, and Z.-N. Qi, “Preparation and properties of organosoluble polyimide/silica hybrid materials by sol–gel process,” *J. Appl. Polym. Sci.*, vol. 73, no. 14, pp. 2977–2984, 1999, doi: 10.1002/(SICI)1097-4628(19990929)73:14<2977::AID-APP22>3.0.CO;2-J.
[22] S.-Y. Fu, X.-Q. Feng, B. Lauke, and Y.-W. Mai, “Effects of particle size, particle/matrix interface adhesion and particle loading on mechanical properties of particulate–polymer composites,” *Compos. Part B Eng.*, vol. 39, no. 6, pp. 933–961, Sep. 2008, doi: 10.1016/j.compositesb.2008.01.002.
[23] T. Huber, M. Misra, and A. K. Mohanty, “The effect of particle size on the rheological properties of polyamide 6/biochar composites,” *AIP Conf. Proc.*, vol. 1664, no. 1, p. 150004, May 2015, doi: 10.1063/1.4918500.
[24] P. Dittanet and R. A. Pearson, “Effect of silica nanoparticle size on toughening mechanisms of filled epoxy,” *Polymer*, vol. 53, no. 9, pp. 1890–1905, Apr. 2012, doi: 10.1016/j.polymer.2012.02.052.
[25] J. Tomaszewska, T. Sterzyński, and K. Piszczek, “Rigid poly(vinyl chloride) gelation in a Brabender measuring mixer. III. Transformation in the torque maximum,” *J. Appl. Polym. Sci.*, vol. 106, no. 5, pp. 3158–3164, 2007, doi: 10.1002/app.26754.
[26] S. Sun, C. Li, L. Zhang, H. L. Du, and J. S. Burnell-Gray, “Effects of surface modification of fumed silica on interfacial structures and mechanical properties of poly(vinyl chloride) composites,” *Eur. Polym. J.*, vol. 42, no. 7, pp. 1643–1652, Jul. 2006, doi: 10.1016/j.eurpolymj.2006.01.012.
[27] A. Licari, F. Monlau, A. Solhy, P. Buche, and A. Barakat, “Comparison of various milling modes combined to the enzymatic hydrolysis of lignocellulosic biomass for bioenergy production: Glucose yield and energy efficiency,” *Energy*, vol. 102, pp. 335–342, May 2016, doi: 10.1016/j.energy.2016.02.083.
[28] S. Naik, R. Malla, M. Shaw, and B. Chaudhuri, “Investigation of comminution in a Wiley Mill: Experiments and DEM Simulations,” *Powder Technol.*, vol. 237, pp. 338–354, Mar. 2013, doi: 10.1016/j.powtec.2012.12.019.
[29] Q. Wang, Z. Huang, and Z. Liu, “Overview of High-Value Reuse and Grinding at Sub-Zero Temperature of Scrap Rubber Tires,” *IOP Conf. Ser. Mater. Sci. Eng.*, vol. 472, p. 012071, Feb. 2019, doi: 10.1088/1757-899X/472/1/012071.
[30] “Standard Test Method for Tensile Properties of Plastics.” https://www.astm.org/d0638-14.html (accessed Mar. 29, 2023).
[31] A. Mohammed and A. Abdullah, “SCANNING ELECTRON MICROSCOPY (SEM): A REVIEW”.
[32] C. Schick, “Differential scanning calorimetry (DSC) of semicrystalline polymers,” *Anal. Bioanal. Chem.*, vol. 395, no. 6, pp. 1589–1611, Nov. 2009, doi: 10.1007/s00216-009-3169-y.

[33] N. Bélanger *et al.*, “Evaluating corn-based biochar as an alternative to carbon black in styrene-butadiene rubber composites,” *Mater. Today Commun.*, vol. 34, p. 105218, Mar. 2023, doi: 10.1016/j.mtcomm.2022.105218.
[34] V. Hristov and J. Vlachopoulos, “Effects of polymer molecular weight and filler particle size on flow behavior of wood polymer composites,” *Polym. Compos.*, vol. 29, no. 8, pp. 831–839, 2008, doi: 10.1002/pc.20455.

Appendices

Appendix A: Particle Size Distributions

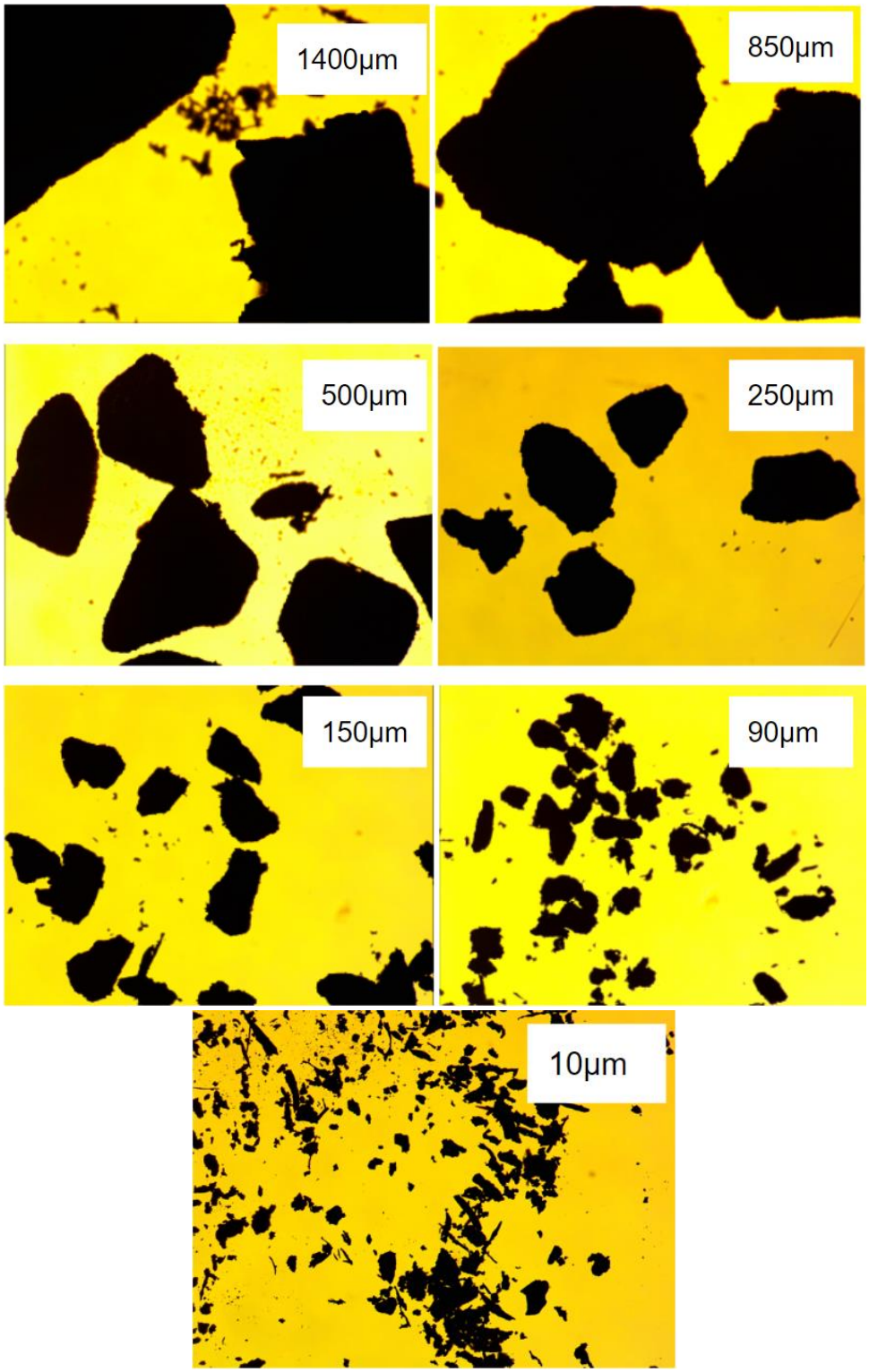

Figure 16: *5x images captured in order of decreasing screen size*

Appendix B: Plastograms and Torque

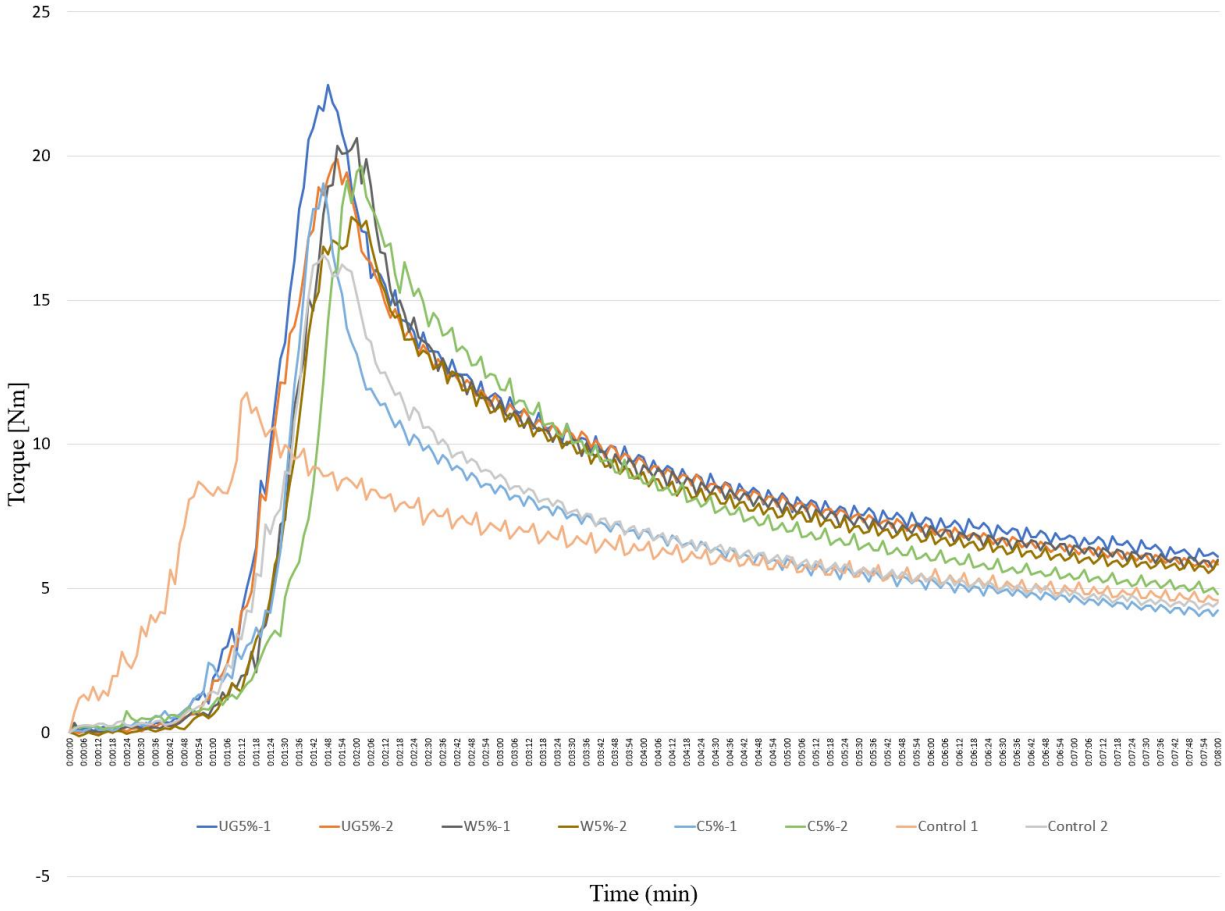

Figure 17: *Plastograms of composites containing 5% BC*

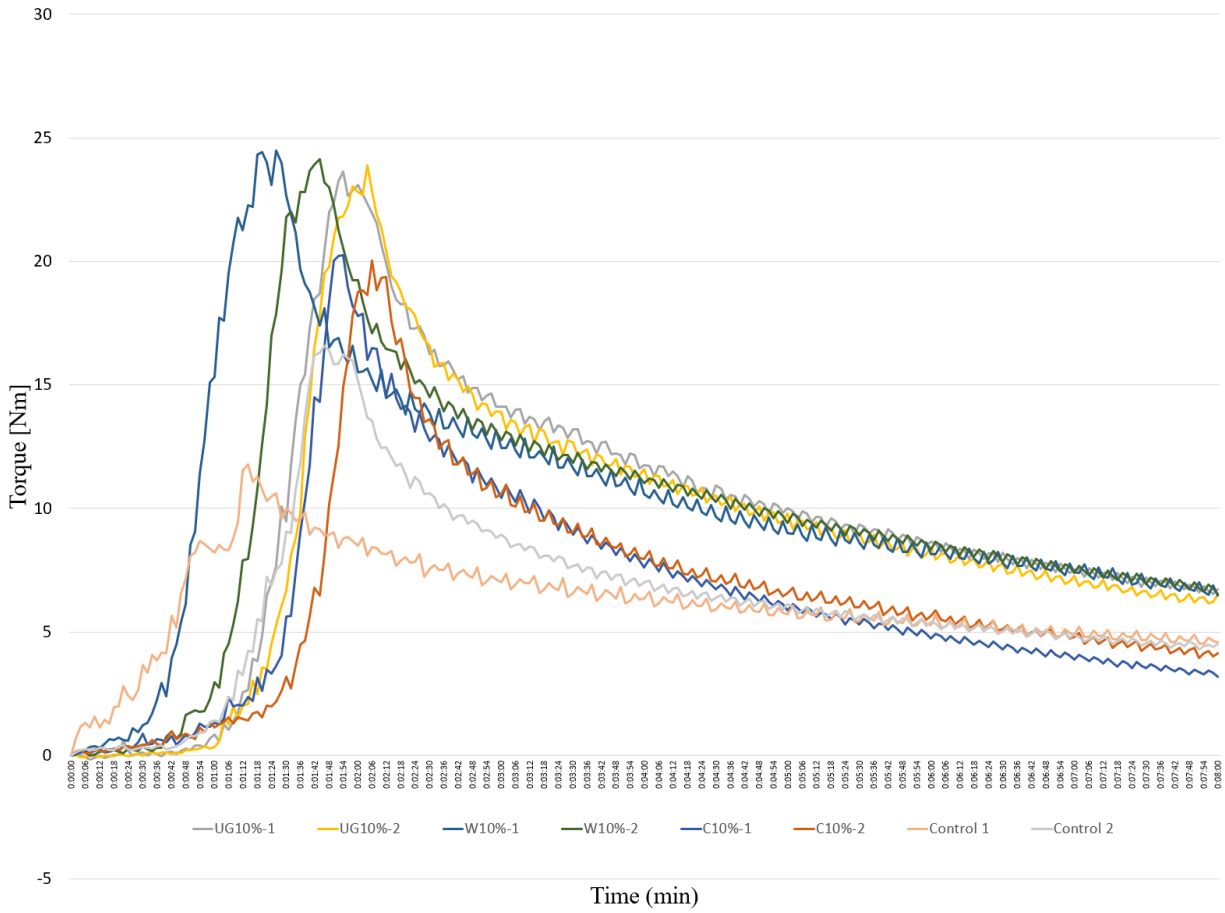

Figure 18: *Plastogram of samples containing 10% BC*

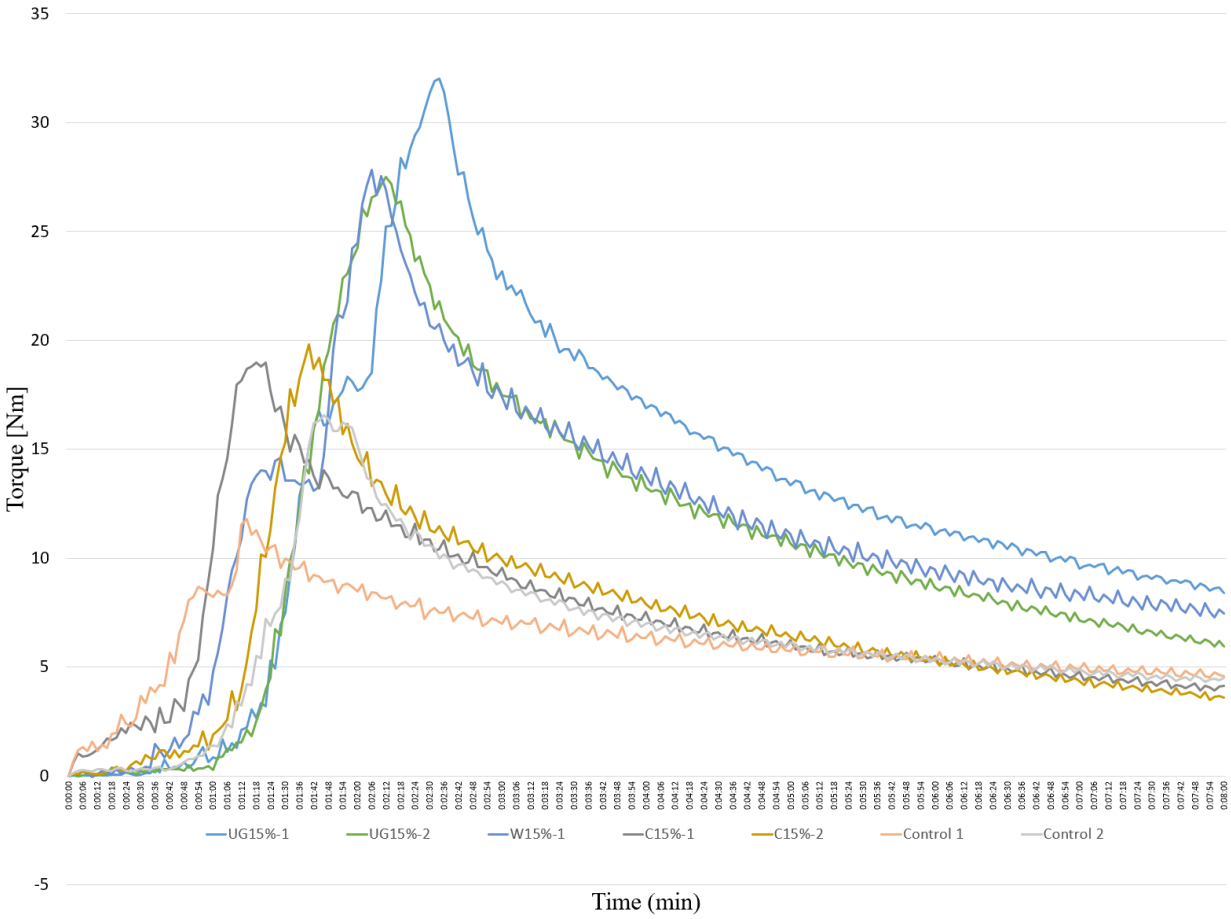

Figure 19: *Plastogram of samples containing 15% BC*

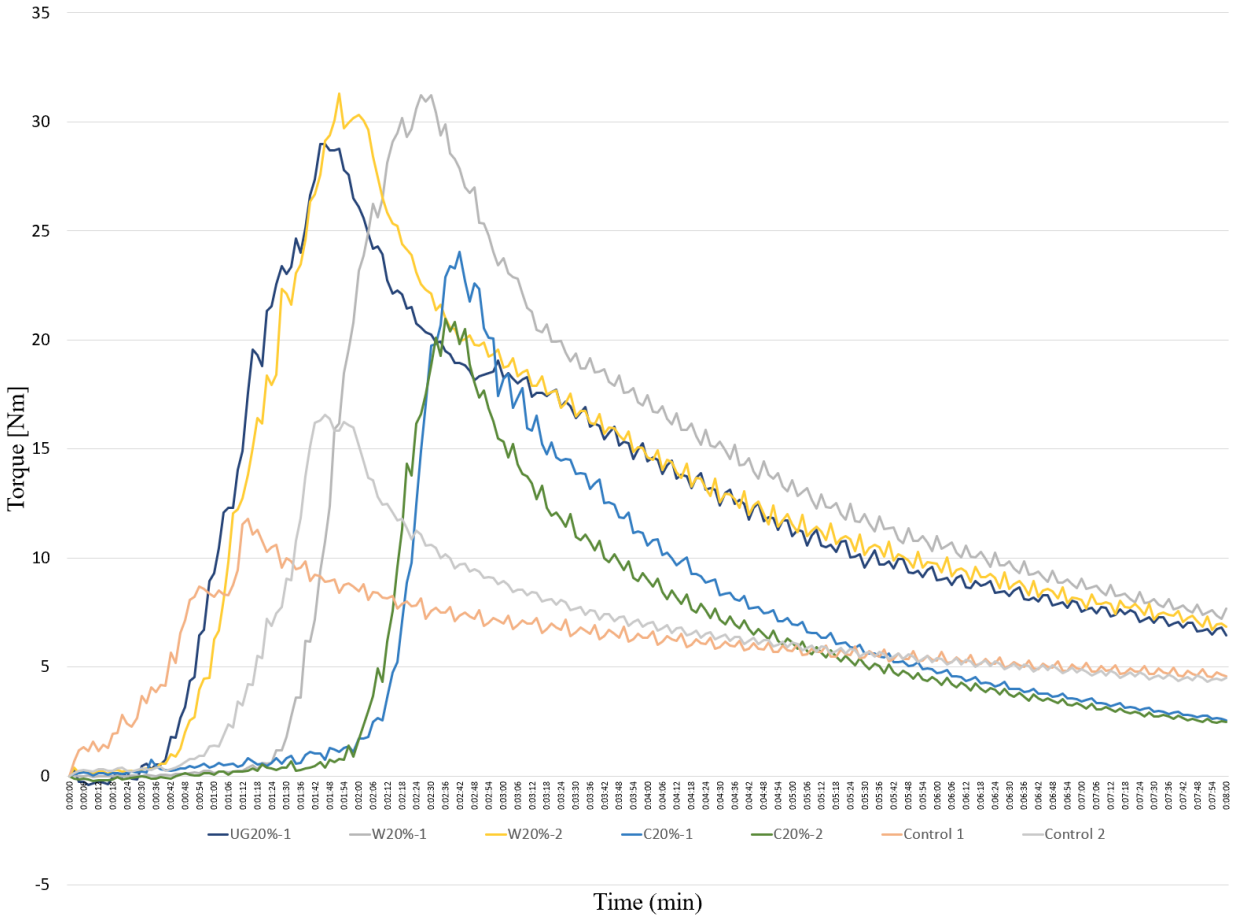

Figure 20: *Plastogram of samples containing 20% BC*

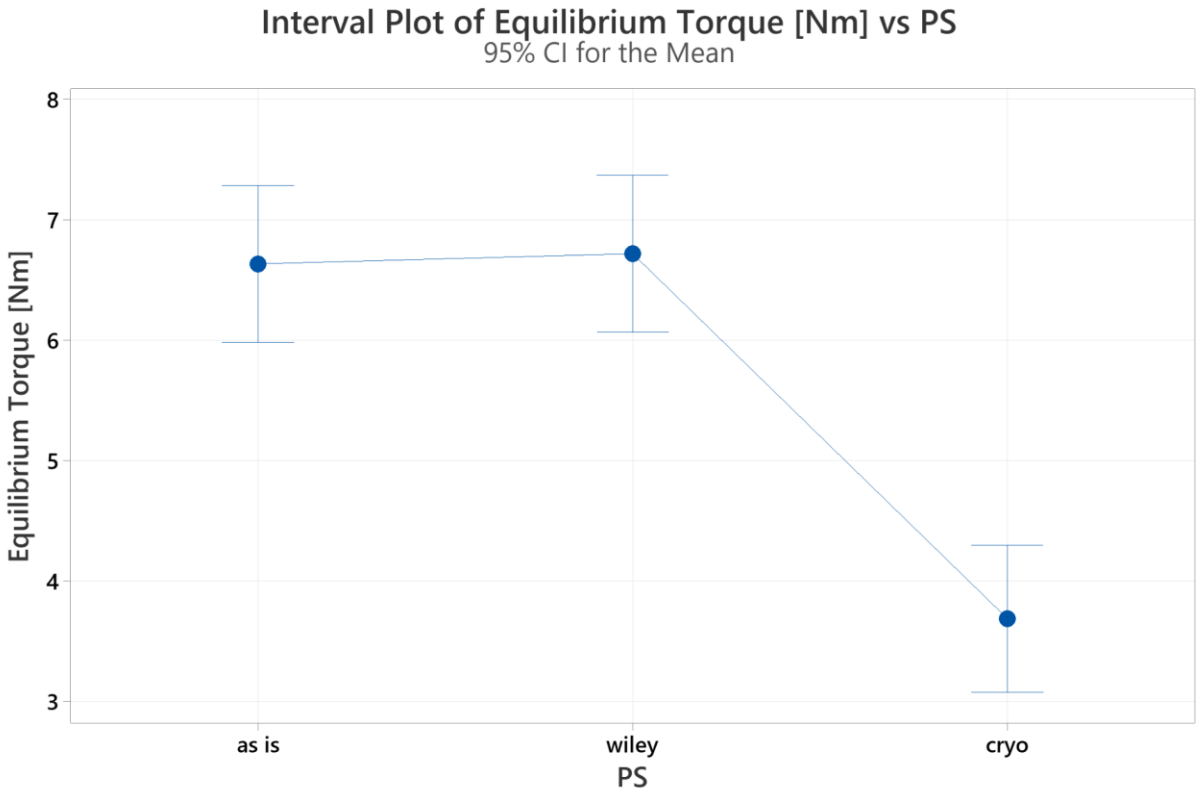

Figure 21*: Equilibrium Torque vs. PS Interval Plot*

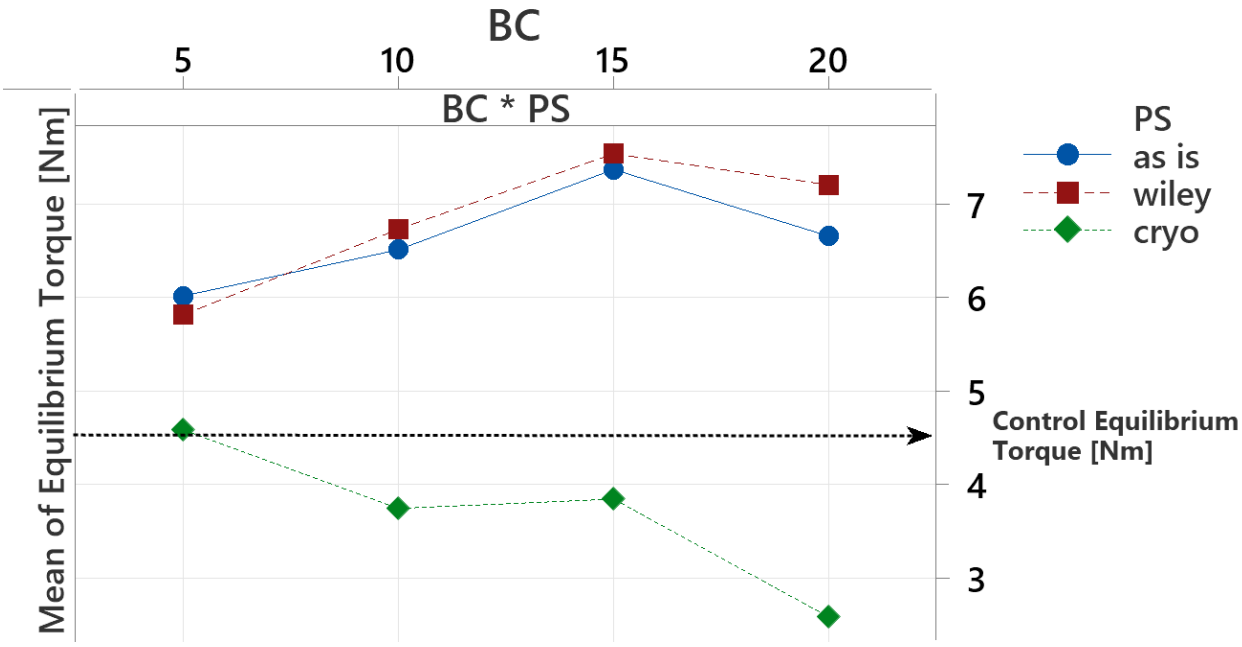

Figure 22: *Equilibrium Torque interaction plot for BC loading and PS*

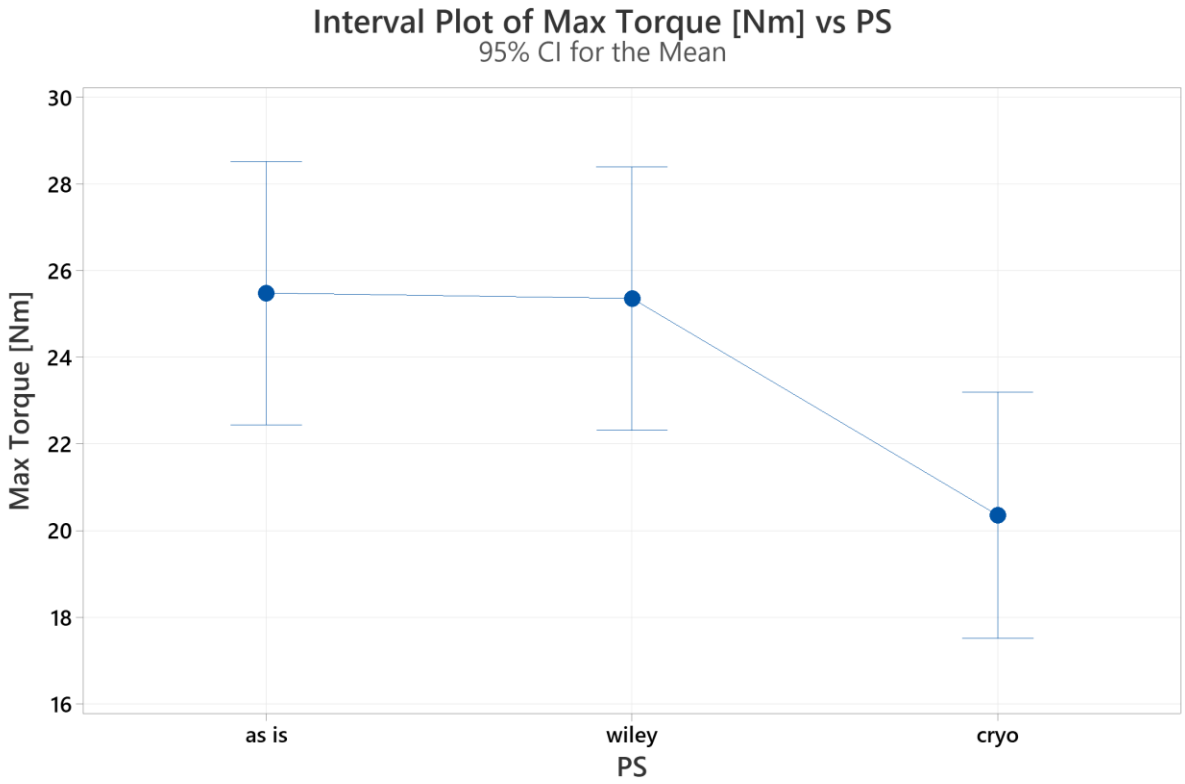

The pooled standard deviation is used to calculate the intervals.

Figure 23*: Maximum Torque vs. PS Interval Plot*

Appendix C: Mechanical Properties

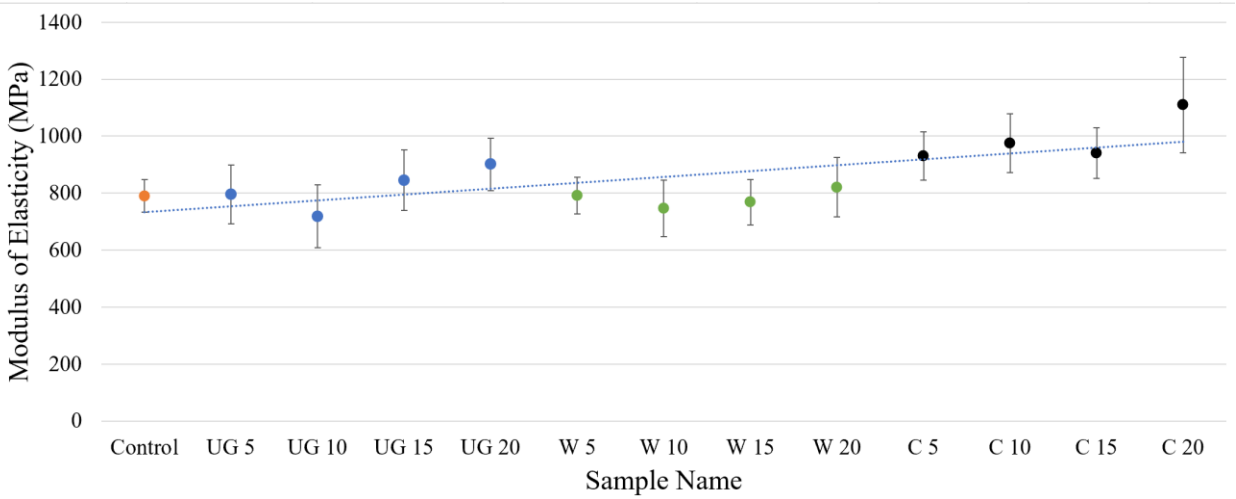

***Figure 24**: Modulus of Elasticity of all samples*

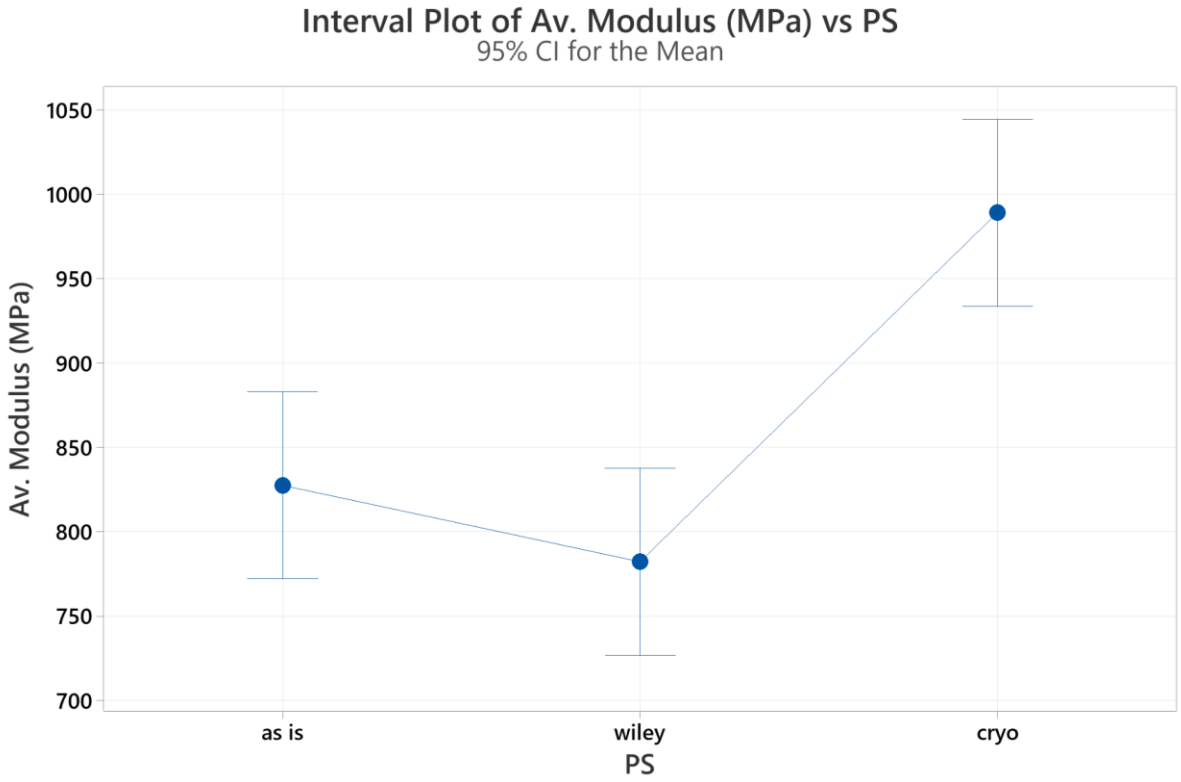

***Figure 25:** Interval Plot of Average Modulus of Elasticity vs. PS*

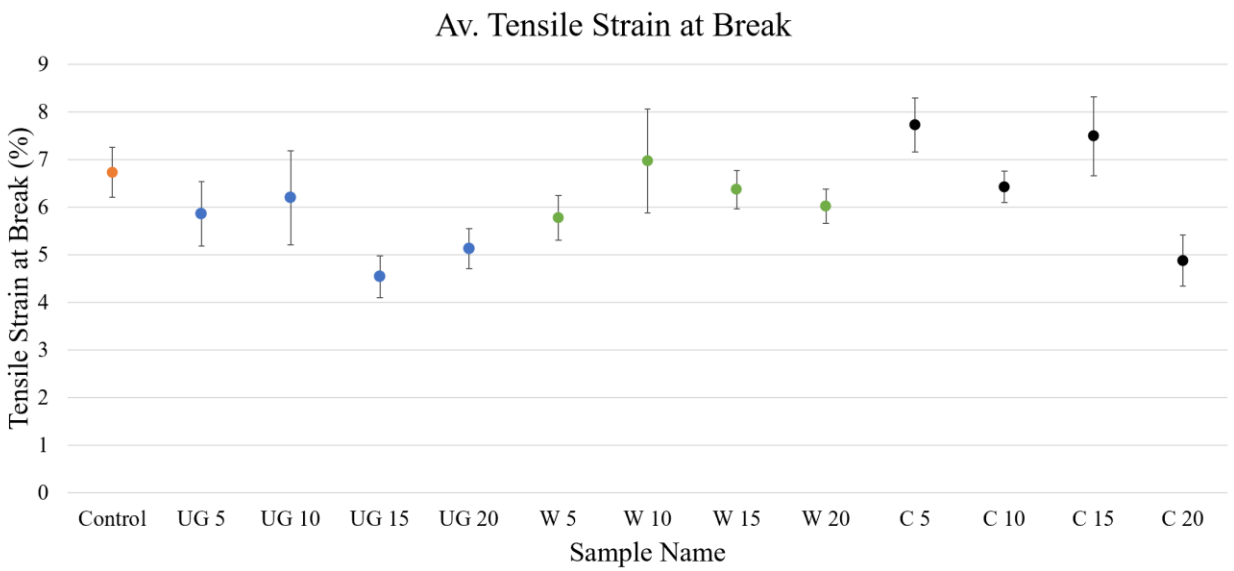

***Figure 26**: Tensile strain at break of all samples*

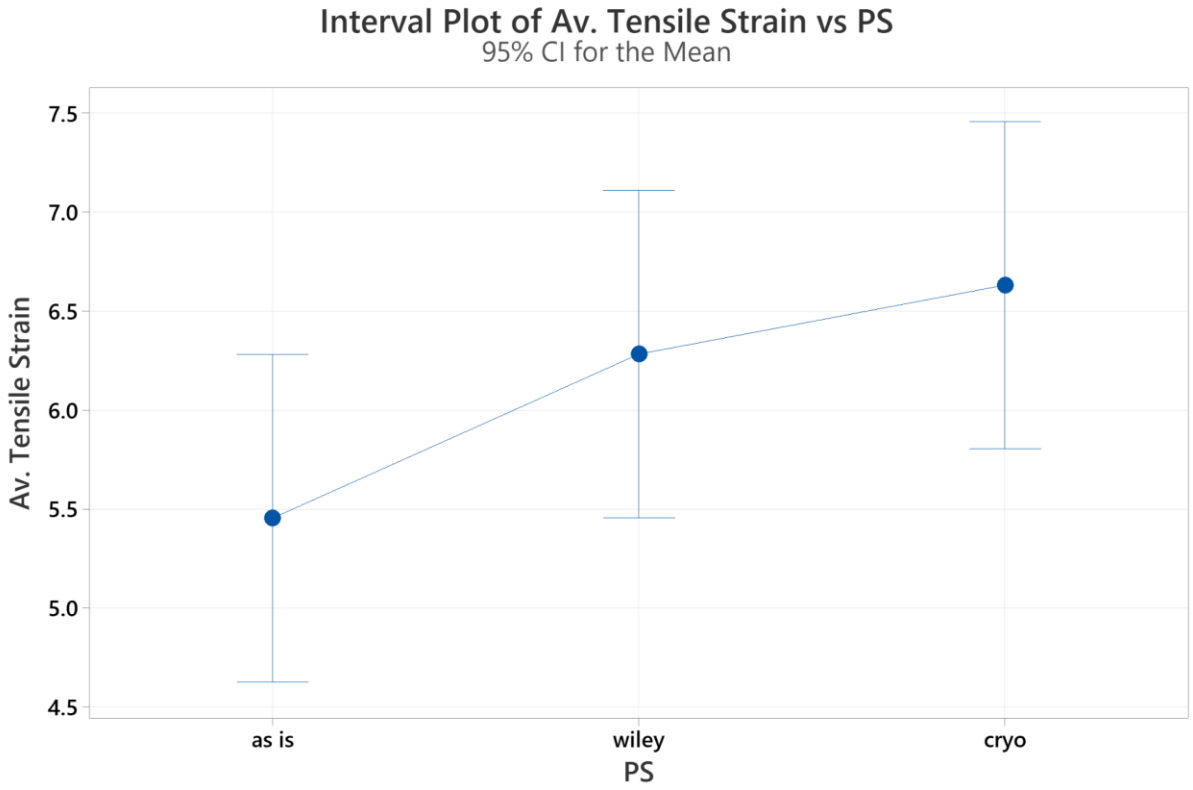

***Figure 27**: Interval Plot for average tensile strain vs. PS*

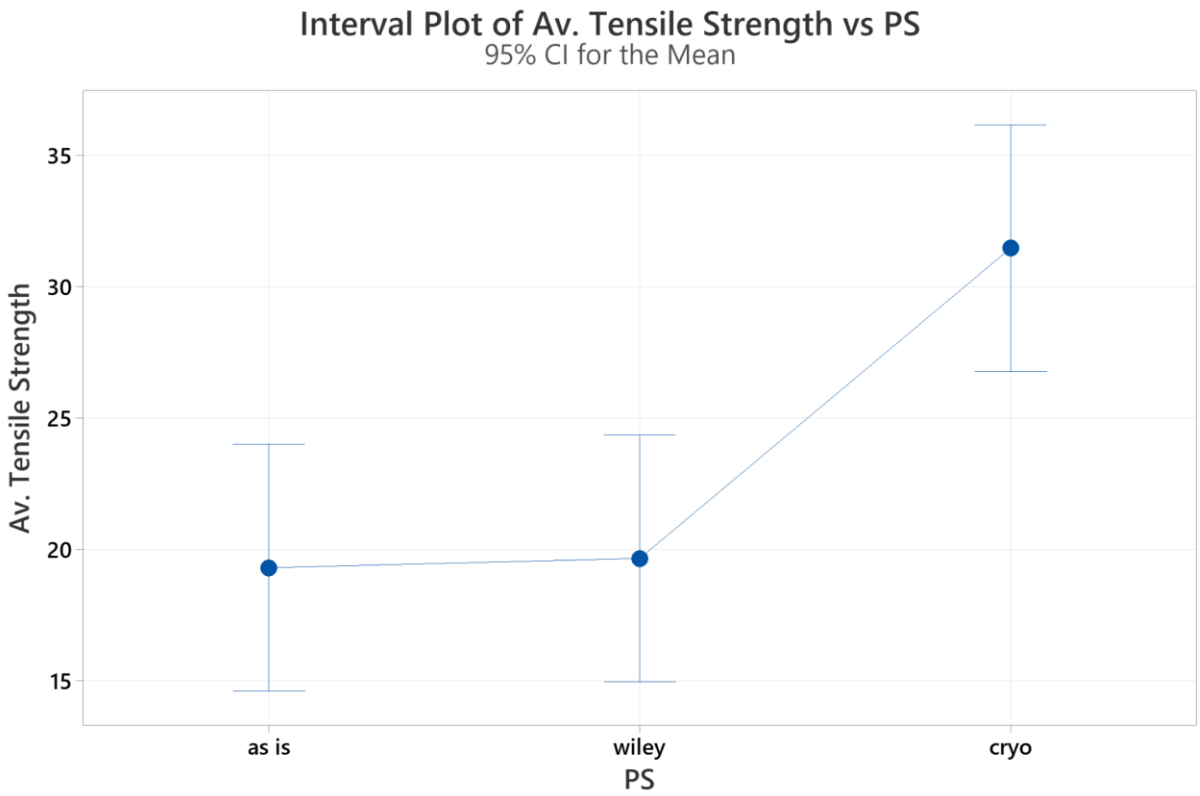

Figure 28: *Interval Plot for average tensile strength vs. PS*

Appendix D: SEM Imaging

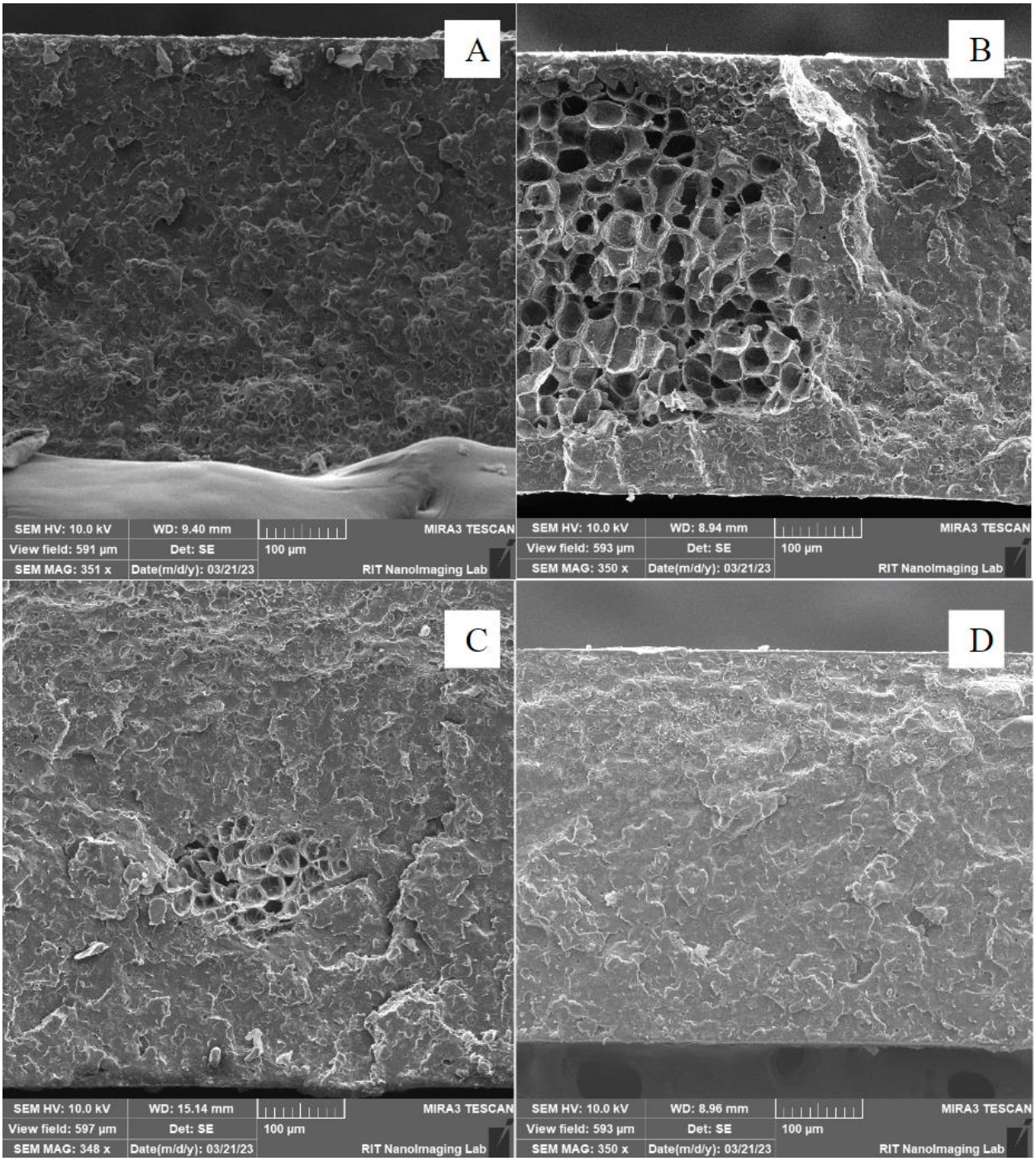

Figure 29: *SEM Imaging at 350x magnification. Samples progress in the following order from left to right; Control (A), Unground 5% (B), TSWM ground 5% (C), Cryo-ground (D)*

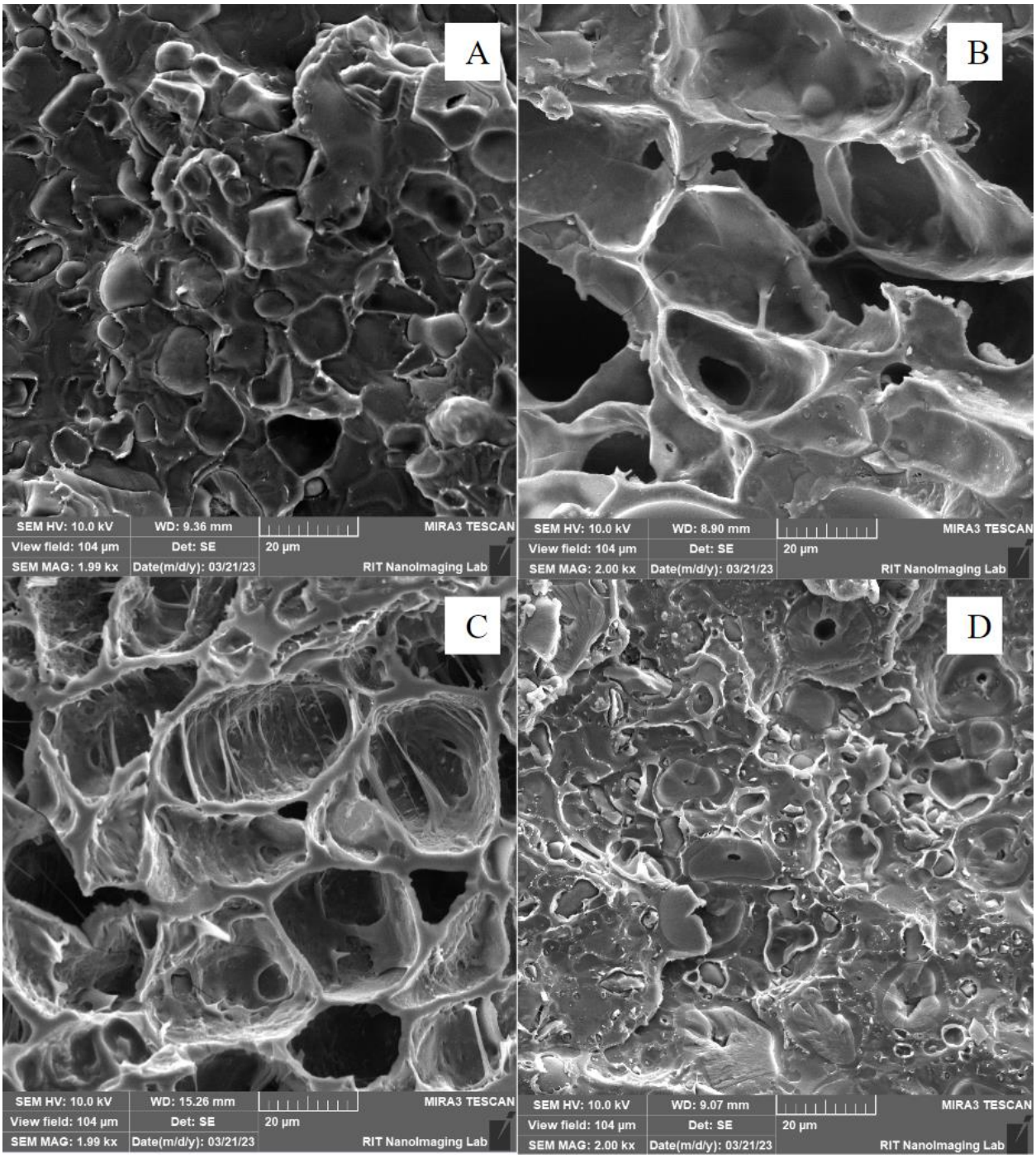

Figure 30*: SEM Imaging at 350x magnification. Samples progress in the following order from left to right; Control (A), Unground 5% (B), TSWM ground 5% (C), Cryo-ground (D)*

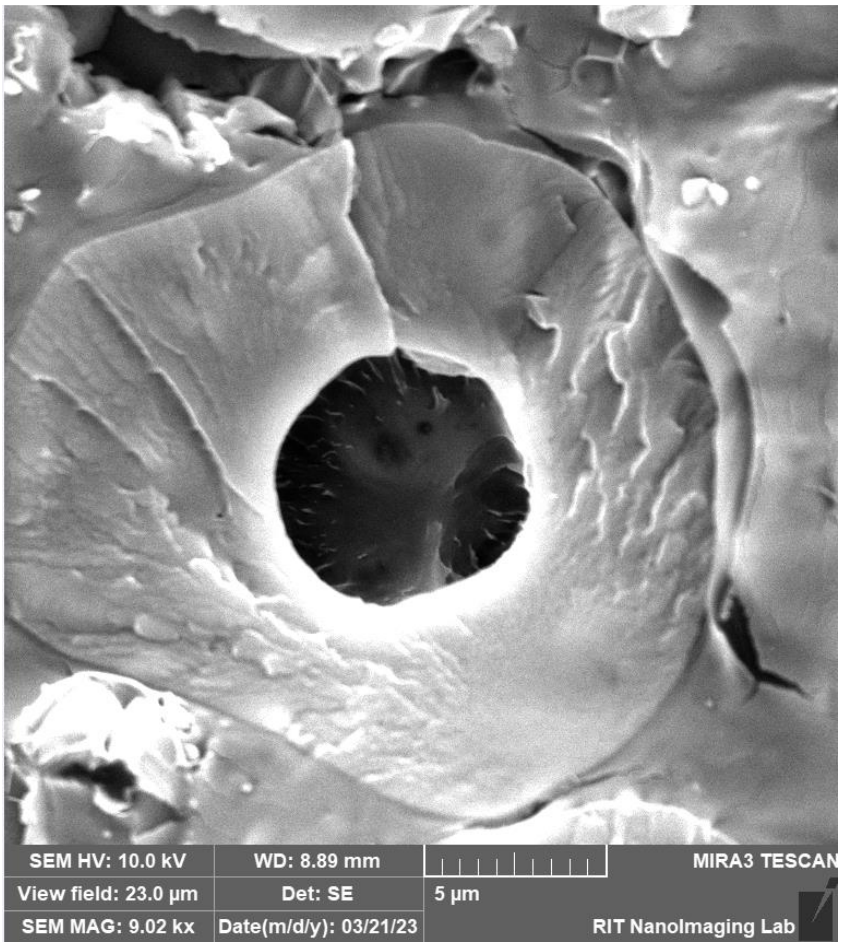

Figure 31: *9000x SEM image that show structure within a hole in cryo-milled sample*

Committee Approval:

Carlos Diaz-Acosta May 12, 2023

Thesis Advisor/ Committee Member/ Observer

Thomas Trabold May 12, 2023

Committee Member/ Observer

Alexis Rich May 12, 2023

Committee Member/ Observer